NASA CONTRACTOR
REPORT

NASA CR-61369

APOLLO 14 COMPOSITE CASTING DEMONSTRATION

Arthur D. Little, Inc.
Cambridge, Mass. 02140

August 20, 1971

Final Report

Prepared for

NASA-GEORGE C. MARSHALL SPACE FLIGHT CENTER
Marshall Space Flight Center, Alabama 35812

FOREWORD

This program was conducted by Arthur D. Little, Inc., for the Product Engineering and Process Technology Laboratory, NASA-MSFC, under Contract No. NAS8-26637. Principal ADL participants in Phase 1--Preliminary Sample Selection--included J. Berkowitz, R. Kent, P. Johnson, J. Milgrom, E. Peters, and A. Wechsler. The evaluation of flight and control samples in Phase 2 was performed by Dr. E. Peters and Mr. P. Johnson, with assistance of Dr. J. Berkowitz, Dr. A. Wechsler and Mr. F. Galligani. Mr. David Marchant of the Massachusetts Institute of Technology assisted in pore distribution measurements.

The guidance, support and suggestions of Mr. H. Wuenscher, I. C. Yates, P. Schuerer, and F. Beyerle of NASA-MSFC throughout the work were instrumental in achieving the desired program results.

TABLE OF CONTENTS

I. SUMMARY

A. PURPOSE AND SCOPE

The objective of this program was to assist the Product Engineering and Process Technology Laboratory, George C. Marshall Space Flight Center, NASA, in the design and implementation of the Composite Casting Demonstration performed during the Apollo 14 mission.

In the first phase of the program, we screened inorganic and organic materials for suitability as simulants for metal matrix and as immiscible liquid composites. We conducted preliminary laboratory tests to determine the solidification behavior, wetting, chemical compatibility and flammability characteristics of selected materials. These materials were not used in the flight test program.

In the second phase, we conducted a post-flight examination and evaluation of Samples 4, 7 and 8 that were processed in space as part of the casting demonstration experiment of Apollo 14; this included a comparison with the earth processed control samples. Our examination consisted of initial characterization, metallographic study by optical and electron microscopy, chemical analysis, X-ray diffraction analysis, and pore size and volume distribution measurements. We conducted laboratory tests to confirm selected observations and made recommendations for performing subsequent composite casting experiments in space. Most of the program effort was devoted to characterization of the flight and control samples.

B. RESULTS

Phase 1 - Candidate Materials

Candidate materials screened included inorganic salt hydrates, salt eutectics, fluorocarbons, organic phosphates and silicates, and low melting organics. Four materials--cobalt nitrate, tri-p-tolylphosphate, decafluorobiphenyl and benzophenone--were selected for laboratory tests. Cobalt nitrate and decafluorobiphenyl were the most promising of these materials. The major potential problem with cobalt nitrate is its chemical reactivity

(ability to act as an oxidizer); decafluorobiphenyl must be more fully evaluated for potential toxicity and flammability.

Phase 2 - Apollo 14 Samples 4, 7 and 8

Sample 4--Copper-Coated SiC Whiskers, Argon Gas, In-Bi Eutectic

The objective of this demonstration was to achieve a uniform distribution of a solid (whiskers) and a gas (argon), both having different densities from the matrix, by directional solidification of the matrix in zero-g. The material would thus consist of a fiber-reinforced foamed eutectic with the eutectic lamellae and the whiskers aligned along the axis of the sample.

Control Sample

The bottom fifth of the sample was fully dense with no SiC whiskers or argon bubbles. There was microstructural continuity across this boundary and the top porous region even though the structures at some distance on either side of the boundary are different. This suggested that this boundary is not due to incomplete melt-back; also, such a planar melt-back interface is not expected from the radial heat source which was employed. This existence of this boundary appears to be the result of gravity separation of the gas bubbles.

The SiC whiskers do not appear to be wet by the molten alloy; most of them were found on the outside surfaces of the sample. The few whiskers located in the matrix were randomly aligned with respect to the eutectic lamellae.

The matrix microstructure within the porous region is quite uniform and exhibits no suggestion of directional solidification. It consists of a mixture of randomly oriented coarse and fine lamellae.

While there were solidification shrinkage pores in the porous region, most of the porosity appears to be gas bubbles. The lack of a shrinkage pipe indicates that a reasonably planar growth interface was maintained throughout, in the macroscopic sense. The interface does not appear to have been planar in the microscopic sense, as evidenced by the microstructure. Many of the pores are surrounded by a number of very small

inclusions which were identified by electron microprobe analysis as an In-Cu intermetallic compound.

Flight Sample

In contrast, the flight sample was very uniform throughout, both in microstructure and in distribution of the gas pores. While a foam (in the strictest sense of the word) was not formed, the gas porosity appears to have maintained a uniform dispersion during the entire time required for solidification in zero-g. The microstructure throughout is similar to that described above for the porous region of the control sample.

Heat appears to have been removed from both ends of the sample. Good contact between the melt and container at both ends led to a necked region near the top of the sample. There is no evidence in the macro or microstructure that solidification was directional. Based upon a uniform pore distribution, solidification in the flight sample appears to have been more uniform than in the control. A considerable number of whiskers were mechanically mixed in the melt. These whiskers were generally clustered within both gas pores and shrinkage pores. The inclusion of whiskers in the flight sample points out a major difference from the control in which the whiskers were rejected from the melt. As in the control, numerous In-Cu precipitates were observed surrounding many of the pores.

Sample 7--In-Bi Eutectic, Argon, Stainless Steel Screen

This sample contained a transverse stainless steel screen which was included to promote gas foaming upon shaking of the melt. The objective of this demonstration was to achieve a uniform distribution of a gas (foam) in a more dense matrix. The directional solidification was intended to provide a lamellar eutectic structure oriented along the axis of the sample.

Control Sample

The control sample had no observable foam or gas porosity, indicating complete separation under gravitation. The macrostructure indicated heat was being extracted through the capsule walls and the screen, as well as

the capsule bottom. The solidification interface had considerable concave curvature. Initially solidified regions exhibit conventional colonies or cells of fine lamellar eutectic, after which the structure degenerates to a coarse random eutectic structure, with the grains or colonies elongated in the direction of heat flow.

Flight Sample

In contrast, the flight sample exhibits some retained porosity. The porosity is approximately 3% in the bottom half and 5% in the top half by volume. It is difficult to ascertain whether this is all gas porosity, or whether some shrinkage porosity may be present. However, in the strict sense, there was no foam.

The melt was very nearly in free-float conditions. The macrostructure reveals that contact with the container, and therefore heat extraction, occurred at only a few random positions. These regions contain a fine lamellar structure in elongated colonies radiating away from the point of contact. In other areas, the structure degenerated as in the control.

An extremely interesting feature of the flight sample are several regions which can best be described as rosettes or flower petals. These consist of a central core consisting of a structure reminiscent of "Chinese script," surrounded by radiating elongated colonies of fine lamellar eutectic which form the petals. The structure degenerates to coarse random lamellae at the outer periphery.

Sample 8--In-Bi Eutectic, Tungsten Spheres, Argon Gas

The objective of this demonstration was to achieve a uniform dispersion of the dense spheres and argon gas bubbles in an aligned lamellar eutectic matrix.

Control Sample

No tungsten spheres were found in the bulk of the control sample. A few spheres were trapped in the matrix of the last material to freeze at the end opposite the chill. The remainder of the spheres were not incorporated into the solidified sample and were found on the external surfaces.

Any of the spheres dispersed in the melt prior to solidification were apparently pushed ahead of the liquid-solid interface because of their non-wetting characteristics or settled out under gravitation.

The macrostructure indicates that freezing did not occur in a planar interface normal to the axis of the sample. There appears to be some independent nucleation at several points on the wall of the container. A number of In_2Bi dendrites were observed in an area of the end opposite the chill. The most likely reason for these is the melt being off the eutectic composition.

Flight Sample

In contrast, a considerable number of the spheres are found within the sample, primarily in the shrinkage pores. As with the other flight Samples 4 and 7, solidification appears to have initiated at a number of sites, so that the pore and sphere distribution was macroscopically quite uniform throughout the sample.

This sample is unique among the No. 4, 7 and 8 samples in that the microstructure has large areas of aligned fine lamellar eutectic typical of the classical directionally solidified eutectics. This is probably the result of the proper combination of alloy chemistry and solidification rate which occurred only in this sample. Several rosette growth structures can also be seen.

C. CONCLUSIONS AND RECOMMENDATIONS

A comparison of the flight and control samples led us to the following conclusions.

- Observation of the macrostructure and microstructure indicate that solidification in both the flight and control samples was not truly directional.
- Even without directional solidification, several interesting structural differences were observed between flight and control samples. (1) Apparent intermittent contact of the melt with the container in the flight samples led to unusual nucleation and growth structures. (2) There was a

greater uniformity--on a macro scale--of both pores and structural features in the flight sample, presumably the result of the reduced gravity conditions.

- Although the spheres and whiskers did not wet the matrix adequately, the flight experiment clearly demonstrated that it is feasible to produce enhanced dispersions of gases and dense phases in a melt which is solidified in reduced gravity.
- The use of whiskers appears to enhance the retention and uniform distribution of gas bubbles.

The analysis of the flight and control samples suggest several modifications or new approaches for future experiments.

- Directional solidification should be improved by using a matrix of high thermal conductivity, and a container of low conductivity walls. A two stage heating/cooling cycle may help directional solidification.
- New sample materials should be selected in which the dispersant fully wets the matrix material.
- Experiments should be conducted in two modes: (a) where the melt is in good thermal contact with the container and (b) where the melt is in a free-float condition.

II. BACKGROUND

Arthur D. Little, Inc., was one of several contractors who assisted the Product Engineering and Process Technology Laboratory, George C. Marshall Space Flight Center, NASA in the design and implementation of a Composite Casting Demonstration performed during the flyback phase of the Apollo 14 mission. This demonstration represented the first opportunity to experimentally assess the potential advantages of processing in space, in particular, to determine the effects of the lack of density segregation (bouyancy) and heat convection in the weightless environment of space.

A series of 18 samples representing four experiment categories were ultimately selected by NASA personnel for this first casting demonstration; 11 of the 18 samples were processed in space.* Several of the samples were melted and resolidified with no intentional agitation to permit evaluation of particle redistribution. The other samples were manually agitated to achieve a reasonable mixture of particles and/or gas bubbles in the liquid phase base material.

A listing of the specimens is presented in Table 1. The four categories represent composite structures which cannot presently be made on earth due to density segregation and convection effects caused by gravitational forces. The basis of composite material selection and demonstration objectives for each of the sample groups has been given by NASA(1) as follows:

> "In Group A, two powder metallurgical samples containing, in one case, an even distribution of tiny tungsten spheres which are about 2-1/2 times heavier than the base metal,

---

*A brief study of alternative sample materials was conducted by Arthur D. Little, Inc., in the beginning of this program. This work is described in Appendix A.

(1)"Fact Sheet - Apollo 14 Composite Casting Demonstration," obtained from H. Wuenscher, Manufacturing Engineering Laboratory, George C. Marshall Space Flight Center.

TABLE 1

SPECIMEN SELECTION LIST FOR APOLLO 14 COMPOSITE CASTING DEMONSTRATION

	Specimen No.	Processing in Weightless Environment
A. Particle Dispersion in Metal Matrix or Model Matrix		
a. W Spheres 30% + InBi Powder Compact	1	Melt and solidify
B_4C Spheres 30% + InBi Powder Compact	3	Melt and solidify
b. W Spheres 30% + InBi	10	Melt, disperse by shaking and solidify
c. BeCu Fibers 6% + InBi	13	
BeCu Fibers 6% + Paraffin	14	
B. Gas + Particle Dispersion in Metal or Model Matrix		
a. Argon 25% + InBi	7	Melt, disperse by shaking and solidify
b. W Spheres 6% + Ar 25% + InBi	8	
W Spheres 30% + Ar 5% + InBi Powder Compact	2	Melt and solidify
c. BeCu Fibers 6% + Ar 25% + InBi	5	Melt, disperse by shaking and solidify
BeCu Fibers 6% + Ar 25% + Paraffin	11	
d. SiC Whiskers + Ar 25% + InBi	4	
C. Immiscible Dispersions		
a. Paraffin 50% + NaAc 50%	6	Melt, disperse by shaking and solidify
b. Paraffin 40% + NaAc 40% + W Spheres 20%	12	
c. Paraffin 40% + NaAc 40% + Ar 20%	9	
D. Solidification of Metal Matrix and Free Casting		
a. Controlled InBi Eutectic Solidification	15	Melt and solidify
b. Single Crystal Solidification InBi	16	
c. Solidification InBi From a Point	17	
d. Free Solidification of Sphere	18	

and in the other case, boron carbide spheres, which are about 3 times lighter than the base metal, are melted and solidified without disturbance in order to study influences to the mixture stability which are not caused by gravity. The other samples are in segregated configuration as a result of the preparation in liquid base metal on earth and the manual shaking by the astronaut should cause distribution of particles in the matrix. The feasibility of particle composites of improved mechanical, optical and electrical properties and suitable for economical casting of precision components in space are the goal of this demonstration.

"In Group B, gas has been added alone and in addition to the particles. The dispersion of the gas should create unique configuration of density controlled and particle reinforced composite materials. It is hoped that the samples will show some spots of interesting internal material combinations. If such configurations can be repeated after more development with the proper base metals and high strength reinforcement particles, a drastic increase in strength-to-weight ratio could result. This group contains also one sample made by powder metallurgy, which will serve as a baseline specimen.

"Group C contains test samples for studying the immiscible metal composite formation. On earth, metal components of different density and which do not form alloys, segregate immediately and emulsions of such metals cannot be achieved in solid state. Therefore, properties of such immiscible composites are subject of future exploration.

"The last Group D concerns the directional solidification of the base metal InBi, where the lack of gravity segregation should improve the intermetallic compound formation in one sample and the single crystal formation in the other samples. The last sample in this group demonstrates surface tension or free casting in weightlessness. A spring-loaded piston

extrudes the liquid metal into a cavity, where it will form a precision sphere without touching the walls of the container."

Several specimens, including all of Group D, were not processed due to limitations in the time available for these experiments during the flyback. Arthur D. Little, Inc., was selected to conduct the post-flight examination and evaluation of Samples 4, 7 and 8, including a comparison to the corresponding earth-processed control samples.

III. SAMPLE PREPARATION AND PROCESSING

A. PREPARATION

The ground control and flight samples were prepared at MSFC, as follows:

Sample 4

	Flight	Control
In-Bi Alloy	89.3 g	90 g
Cu-Coated SiC	1.5 g	1.5 g
Argon	25% (volume)	25% (volume)

The In-Bi and SiC whiskers were premixed in a plastic dish. The mixture was heated to a liquid and poured into the capsule to the three-quarter mark. The mix was allowed to cool (solidify) on a heat sink. The capsule was placed in a vacuum, evacuated, then back-filled with argon. The top disk, with its O-ring, was pressed into the capsule to seal in its contents. After cleaning, the capsule top was electron beam welded.

Sample 7

	Flight	Control
In-Bi Alloy	100.6 g	103.9 g
Stainless Screening	6.3 g	5.7 g
Argon	25% (volume)	25% (volume)

The In-Bi was melted and poured into the capsule to the three-quarter mark. The preheated stainless steel screen was inserted while the alloy was in a liquid state. The capsule was evacuated, back-filled with argon, capped, sealed and welded.

Sample 8

	Flight	Control
In-Bi	99 g	99 g
Cu-Coated W	21 g	21 g
Argon	25% (volume)	25% (volume)

The copper coated tungsten spheres were weighed and placed in the capsule. The In-Bi was melted and poured into the capsule to the three-quarter mark. After the alloy had solidified, the capsule was evacuated, back-filled with argon, capped, cleaned and welded.

All of the samples were X-rayed to detect flaws, voids or discontinuities in the weld and were leak checked.

B. SAMPLE PROCESSING

The samples were processed in an apparatus which included an electrical heater and a storage box for the heater which also served as a heat sink for cooling the samples.[2] Samples 4, 7 and 8 were heated for 10 minutes and were then agitated as follows:

(1) Remove heater (containing specimen capsule) from box and, holding firmly in one hand, bump ends alternately against heel of other hand, four times each end.

(2) Perform the following sequence three times:

a. Linear shakes, vigorously, 10 back-and-forth shakes.

b. Oscillate rapidly through at least 15 back-and-forth cycles by turning wrist at least 180°.

[2] A complete description of the apparatus is given in "Report on Results of Apollo 14 Composite Casting Demonstration," I. C. Yates, Marshall Space Flight Center, NASA, S&E-PT-IN-71-1, July 13, 1971.

(3) Oscillate vigorously a few times, then slow down gradually over 10 cycles to very slow motion (5 seconds per cycle).

(4) Carefully move to heater and insert on cooling pan.

(5) Allow to cool 30 minutes minimum.

Simulated heating and shaking cycles were instrumented at MSFC and yielded the results presented in Figures 1 and 2. For these experiments, the sample was molten for a period of 12 to 15 minutes. The sample agitation sequence required approximately 2 minutes.

IV. PRELIMINARY SAMPLE EVALUATION

Arthur D. Little, Inc., staff attended and viewed the opening and preliminary characterization measurements of Samples 4, 7 and 8 at MSFC on April 14 and 15, 1971. The contractor-designated portions of these samples were then hand-carried back to Arthur D. Little, Inc., laboratories for detailed evaluation.

A comprehensive Operations Plan and Procedures for Evaluation was prepared by the Product Engineering and Process Technology Laboratory, MSFC to provide for accountability, transfer and storage of samples, preliminary evaluation plans including specimen opening and sectioning, and final evaluation plans to be conducted by the contractors. Several portions of this document relating to preliminary characterization steps are reviewed below.

- Specimen Identification

The samples will be identified by a specimen number (as given in Table 1), process condition (flight, control or spare), longitudinal section (arbitrarily designated half A and half B) and subsection number. As an example, 4F-A-02 would represent piece number 2 from the contractor's half of the experiment number 4 flight sample.

- Initial Characterization

Prior to capsule opening, the various specimens were radiographed to provide shadow graphs of the sample distribution within the capsule. These radiographs are presented in the detailed sample description later in this report.

Additionally, it was feared that the samples containing argon gas were altered during the capsule sealing (welding) process, providing a vacuum rather than argon atmosphere. Prior to capsule opening, the capsules were accurately weighed to 0.1 milligram; the containers were then pierced and reweighed. The results for Samples 4, 7 and 8 were:

Weight (grams)	Sample 4C	4F	7C	7F	8C	8F
After Piercing	119.1394	120.4633	141.0280	137.8113	150.8099	151.2974
Before Piercing	119.1380	120.4627	141.0299	137.8103	150.8037	151.2943
Difference (mg)	+1.4	+0.6	-1.9	+1.0	+6.2	+3.1

As the volume of the specimen capsules corresponds to about 25 cc, 25 volume percent argon would correspond to 10.9 mg (at 1 atm). For a weighing uncertainty of $\pm$ 2 mg, it is clear that as much as 25% of the original argon has been lost from sample 8F and up to 50% lost from sample 8C.

- Capsule Opening Procedure

The capsules were opened by carefully machining in a lathe down to a wall thickness of 0.005 in. A 10-pitch thread was then formed on the side wall of the capsule, after which the end of the capsule was removed. Finally, the threaded metal shell was unwrapped from the sample.

After the specimens were removed from the capsule, they were weighed and dimensions were measured. These data are reported in Table 2. Photographs were obtained of the specimens at 0° and 180° aspects and of specimen tops and bottoms.

The specimens were then held in a specially prepared jig and were manually sectioned with a hacksaw into two longitudinal sections, one of which was furnished to the contractor and the other being retained at MSFC. Photographs were taken of the sectioned pieces.

TABLE 2

DATA SHEET FOR PROCESSED COMPOSITE CASTING SAMPLES 4, 7 AND 8

	4C	4F	7C	7F	8C*	8F*
Initial Weight (g)	91.5	90.8	109.6	106.9	120.0	120.0
Weight of Slug (g)	88.0	89.3	109.7	106.7	102.1	116.4
Length of Slug (cm)	5.59	7.62	5.65	7.62	5.97	7.42
Diameter of Slug (cm)	1.753	1.755	1.750	N/A	1.748	1.687
Center of Gravity from Bottom (cm)	2.54	3.07	2.93	3.70	2.79	3.37

*The large difference between initial and final weights is due to the rejection of tungsten spheres from the alloy slug. Based upon the initial weight of tungsten (21 grams for each sample) and the weight difference after processing, Sample 8C contains a maximum of 15% of the tungsten spheres (most of which adhered to the outer surface of the slug) and Sample 8F, 83% of the tungsten spheres.

V. DETAILED SAMPLE EVALUATION

This section contains:

- A brief description of the experimental techniques used to characterize the samples;
- The results of these characterization studies for each of the three flight and three control samples; and
- A description of several experiments performed in our laboratories to supplement or support the observations made on the samples.

The results are presented separately for each of the three systems. While this leads to some repetitiveness where observations pertain to more than one system, each of the three sections is thus complete in itself.

A. EXPERIMENTAL PROCEDURES - SAMPLE CHARACTERIZATION

1. Radiography

Radiographs of the unopened sample capsules were provided by NASA. These were taken at 55 kv and 5 ma for 6 minutes. Exposure was on Type M film with a 48-in source to specimen distance.

2. Metallography

a. Sectioning

Samples were sectioned by cooling them in LN_2 and then sawing with a jeweler's saw.

b. Mounting

The majority of samples were prepared metallographically without mounting. A few samples were mounted without degradation of the sample in a cold curing resin (Trade name "Koldmount").

c. Polishing

Grinding was carried out on wet silicon carbide papers, 400 and 600 grit successively. Rough polishing was done with 6 micron diamond on a

beeswax lap, wet with methanol. Final polish was on a wet napped synthetic rayon cloth using 1 micron diamond. The only major difficulty encountered was continued gouging of the No. 8 specimens by pulled-out tungsten spheres, preventing the attainment of scratch-free samples.

d. Etching

We used the following etchant:

Hydrochloric acid	10 cc
Picric acid	2 cc
Ethyl alcohol	200 cc

Application was by immersion for 10-20 seconds. Often, alternate etching and polishing was required. This etch attacks the indium bismuth solid solution and leaves the In_2Bi intermetallic light-colored in the optical microscope.

3. Chemistry

The chemistry of the matrix was determined by emission spectrographic analysis. Electron microprobe analysis was used to identify the two major metallic phases in the matrix with respect to their appearance optically and to determine the major elements present in inclusions.

4. X-ray Analysis

Laue back reflection techniques were used to ascertain qualitatively the degree of polycrystallinity and preferred orientation of the eutectic matrix. The Laue patterns were obtained on Polaroid Type 57 film using a copper tube at 40 kv and 20 ma with a 3-minute exposure.

X-ray diffraction was used to identify the crystallographic phases present. Diffraction scans were made with copper K_α radiation at 40 kv and 20 ma.

5. Fracture Surfaces

One sample (No. 7F) was fractured at the stainless steel screen in order to observe bubble distribution in this area. An attempt was made to do this in a tensile tester, but the sample broke in this plane while being handled after being cooled down.

6. Bubble and Pore Distribution

These were measured on a traveling stage quantitative microscope using the chord-intercept technique. The work was performed by David D. Marchant of the Massachusetts Institute of Technology.

B. RESULTS

1. Sample 4

The No. 4 samples contained copper coated SiC whiskers, argon gas, and the In-Bi eutectic matrix. The objective of this demonstration was to achieve a uniform distribution of a solid (whiskers) and a gas (argon), both having different densities from the matrix, by directional solidification of the matrix in reduced gravity. The material would thus consist of a fiber-reinforced foam eutectic with the eutectic lamellae and the whiskers aligned along the axis of the sample.

a. Radiographs

Figures 3 and 4 are radiographs at 0° and 90° of the control and flight sample capsules, respectively. The down direction for the control sample, and the heat sink position in both cases, is at the bottom of the picture. The solid is in contact with the capsule walls and bottom in the control sample. Some scattered solid is on the walls above the bulk of the sample. The flight sample is in contact with both ends of the capsule. There is a minor neck near the heat sink end and a major neck at the opposite end where there is no contact with the walls.

b. Samples After Removal From Capsule

Figures 5 through 7 are photographs of the samples after removal of the capsule. The major neck near the hot end of the flight sample is quite evident. In addition, the shiny appearance of the bottom end of the control and both ends of the flight sample confirms the radiograph observation that the solid was in contact at these ends.

Figure 8 presents photographs of the No. 4 samples after the first longitudinal sections. The saw markings have obliterated most of the internal structural details.

c. Structural Observations

No. 4 Control

Figure 9 is a schematic of the sections which were taken of Sample 4C-A. Figure 10 indicates the macrostructure of Section 4C-A-00. Approximately the bottom fifth of the sample is fully dense with no SiC whiskers or argon bubbles. The macroscopic structure in this region indicates very good directionality of heat flow toward the heat sink at the bottom. The microstructure in this region varies from a coarse, randomly oriented lamellar structure near the chill (Figure 11a) to a small region of cellular eutectic near the middle of the zone (Figure 11b). The cells are elongated and oriented longitudinally, as would be expected. At the top of the fully dense area there is a regular, but degenerate, eutectic structure somewhat reminiscent of the "Chinese script" structure observed in some other eutectic alloys (Figure 11c). This may indicate a breakdown of planar growth interface stability due to the prevailing thermal and chemical conditions of the melt.

There is microstructural continuity of a sort across the boundary between the bottom of the sample and the top porous region even though the structures at some distance on either side of the boundary are different (Figure 11d).

This suggests that this boundary is not the result of an incomplete melt-back during processing. Also, one would not expect such a planar melt-back interface from the radial heat source which was employed. The existence of this boundary appears more likely to be the result of gravity separation of the gas bubbles. That many bubbles remain at all is surprising during experiments on earth in 1-g because of the low viscosity of the In-Bi alloy when molten. However, it would appear that the SiC whiskers have in some way significantly increased the apparent viscosity of the melt and impeded the upward travel of the gas bubbles. The fact that the whiskers seem to be clustered on the inside surface of the bubbles may be a related occurrence.

The matrix microstructure within the porous region is quite uniform and exhibits no suggestion of directional solidification (Figure 12). It consists of a mixture of randomly oriented coarse and fine lamellae. The bimodal distribution of lamellae widths indicates that this is a real effect and not just the result of the angle of intersection of the structure and the metallographic surface. Examination of a transverse section (4C-A-03T) supports this observation.

While there are some solidification shrinkage pores in the porous region, most of the pores appear to be gas bubbles. The increased porosity near the top of the sample indicates that most of the shrinkage was accommodated there. The lack of a shrinkage pipe indicates that a reasonably planar growth interface was maintained throughout, in the macroscopic sense. As has been mentioned, the interface does not appear to have been planar in the microscopic sense, as evidenced by the breakdown from a lamellar eutectic structure.

There are a number of very fine inclusions or precipitates present in the porous portions of the sample; they tend to be clustered near the pores. This material has been identified by electron microprobe analysis as an In-Cu intermetallic compound.

No. 4 Flight

Figure 13 is a schematic of the sections which were taken of sample 4F-A. Figure 10 indicates the macrostructure of Section 4F-A-00.

The flight sample is very uniform throughout, both in microstructure compound and in distribution of the gas pores. While the gas pores did not foam in the strictest sense of the word, the gas porosity appears to have maintained a uniform dispersion throughout the time required to solidify in reduced gravity. The microstructure throughout is similar to that described above for the porous region of the control sample.

Heat appears to have been removed from both ends of the sample, so that in reduced gravity there was apparently good contact between the melt and container at both ends. This led to the necked region. However, it does not appear that two growth fronts converge in this neck (Figure 14).

There is no evidence in the macro or microstructure of directional solidification. Solidification in the flight sample appears to have been more random or uniform than in the control, since much more shrinkage porosity can be observed distributed uniformly throughout the flight sample. Shrinkage porosity can be distinguished from the gas porosity in general since it appears less regularly spherical in shape.

The whiskers do not appear to be wet by the molten alloy, since most of them ended up on the outside surfaces of the sample, on the gas pore surfaces or on the shrinkage pore surfaces (Figure 15a). In this context, the few whiskers which could be located in the matrix were aligned, if anything, normal to the eutectic lamellae (Figure 15b). It had been predicted that wetting whiskers might align themselves with the lamellae. A considerable number of whiskers were mechanically mixed in the melt as shown by the large number of whiskers observed in the shrinkage pores.

The flight sample also contains a dispersion of In-Cu intermetallic compound inclusions similar to that in the porous region of the control sample.

d. Porosity

Pore density and pore size distribution measurements were performed to evaluate differences between the flight and control samples. The selected specimen traverse lines and measured pore densities are illustrated in Figure 16. The flight sample exhibits a pore density approximately twice that of the control sample. Furthermore, the pore density is rather uniform across the sample, varying from 16% near the bottom to 19% at the top. In contrast, the control sample exhibits considerable variation, being 13% near the bottom of the pore-containing region of the sample and 5% at the top. Based upon measured changes in volume upon solidification, shrinkage pores could not account for more than 2 or 3% of the observed pore density.

We interpret these results as follows. A distribution of argon bubbles was achieved in the molten Bi-In alloy during the agitation stage of sample processing; the argon bubbles accounted for a minimum of 15% of the sample volume. The bubbles migrate to and became attached to SiC fibers (or fiber bundles) as a consequence of the system reducing its

surface free energy, thereby greatly decreasing the mobility of the bubbles. In the case of the flight sample, a few of the bubbles undoubtedly migrated to the outer walls and were annihilated; the rest were frozen into the structure during solidification. In Sample 4C, processed on earth, the bubble distribution is a consequence of the competing rates of solidification vs. bubble migration due to buoyancy. Initially, when there is high heat transfer, solidification proceeds more rapidly and tends to trap in the argon bubbles.* At a later point in time, when heat must be transferred through the solidified In-Bi shell, the rate of solidification is reduced and there is a longer opportunity for bubbles to rise and be removed from the sample.

The pore size distributions for the samples are presented in Figures 17 to 19. Both samples have an average pore size of 60 μm; the flight sample has a more extensive range of sizes.

e. Chemistry

Qualitative emission spectrographic analysis of chips from Sample No. 4F-A indicates no particular decrease in the purity of the matrix elements (Table 3). The low copper content is further indication of the fineness and wide dispersion of the In-Cu intermetallic inclusions.

An X-ray diffraction pattern was obtained from Sample 4F. There are approximately equal quantities of α-In and In_2Bi. There is no evidence of Cu, Al, SiC, or any of their compounds.

2. Sample 7

The No. 7 samples contained the In-Bi eutectic alloy and argon. In addition, the container contained a transverse stainless steel screen to assist in foaming the gas upon shaking of the melt. The objective of this demonstration was to achieve a uniform distribution of a gas (foam) in a more dense matrix. The directional solidification was intended to provide a lamellar eutectic structure oriented along the axis of the sample.

*The fully dense zone corresponding to the bottom 15% of Sample 4C is anomolous and cannot be explained.

TABLE 3

QUALITATIVE EMISSION SPECTROGRAPHIC ANALYSIS
OF SAMPLE 4F-A-00

Element	Amount Present
In, Bi	10-100%
Al, Ag, Pb, Si	3-30 ppm
Cu, Cr, Fe, Ni, Sn	1-10 ppm
Ca, Mg	0.3-3 ppm
Mn	0.1-1 ppm

a. Radiographs

Figures 20 and 21 are radiographs at 0° and 90° of the control and flight capsules, respectively. The down direction for the control sample, and the heat sink position in both cases, is at the bottom of the picture. The control sample contacts the bottom of the capsule, the walls of the capsule, and the stainless steel screen support arms. The flight sample is in contact only at isolated sections of the capsule walls. This pattern is consistent with the macrostructures observed for the two samples (see below).

b. Samples After Removal From the Capsule

Figures 22 through 24 are photographs of the samples after removal from the capsules. These confirm the comments relative to contact of the sample with the capsule.

Figure 25 presents photographs of the No. 7 samples after the first longitudinal sections. The saw has obliterated most of the internal structural details.

c. Structural Observations

No. 7 Control

Figure 26 is a schematic of the sections which were taken of Sample 7C-A. Figure 27 is the macrostructure of Section 7C-A-00.

The control sample had no observable foam or gas porosity, indicating complete separation under gravitation. (This also suggests again that the whiskers in the No. 4 samples did have some effect on the apparent viscosity of the melt.)

The macrostructure in this case also indicates heat was being extracted from the walls and the screen, as well as the bottom. The growth interface had considerable concave curvature. In this regard, growth appears to have initiated at the bottom, the walls, and the screen. These regions exhibit conventional colonies or cells of fine lamellar eutectic (Figure 28a), after which the structure degenerates to a coarse "Chinese script" structure, the grains or colonies elongated in the direction of heat flow (Figure 28b).

No. 7 Flight

Figure 29 is a schematic of the section which were taken of Sample 7F-A. Figure 27 is a macrograph of Section 7F-A-00.

In contrast to the control sample, the flight sample does exhibit some retained porosity. The porosity is approximately 3% in the bottom half and 5% in the top half by volume. It is difficult to ascertain whether this is all gas porosity, or whether some shrinkage porosity may be present. There is, however, no foam. A series of scanning electron micrographs of the fractured surface adjacent to the stainless steel screen are presented in Figure 30. These pictures reveal the presence of many pores.

The melt was very nearly in free-float conditions. The macrostructure reveals that contact with the container, and therefore heat extraction, occurred at only a few places. These regions contain a fine lamellar structure in elongated colonies radiating away from the point of contact. After that, degeneration of the structure occurs as in the control.

One extremely interesting feature of the flight sample is the existence of several regions which can best be described as rosettes or flower petals (Figure 31). These have a central core consisting of a structure reminiscent of "Chinese script" (Figure 32a), surrounded by radiating elongated colonies of fine lamellar eutectic (Figure 32b). These form the petals. The outer periphery occurs as the structure degenerates to coarse random lamellae. It is difficult to establish unequivocally the sequence of events leading to the formation of these rosettes. It may be that the script area nucleated on the container wall, broke loose, and then floated in the melt as a particle for a time. Subsequent growth may have occurred as the melt became constitutionally or thermally supercooled. After growth proceeded for a time, the structure became degenerate, possibly due to a change in growth conditions, such as that which could have been caused by the latent heat released by the growing rosette.

d. X-ray

X-ray Laue back reflection patterns were obtained from both the outer surface of 7F and Section 7F-A-00.

The surface of 7F (which was the brightest and shiniest at the time of opening) is polycrystalline. There is a preferred orientation to the structure as evidenced by the presence of diffraction arcs (rather than full rings that would be obtained from random orientation). The 7F-A-00 surface provided a multitude of spots, indicating a contribution from two or three areas of uniform orientation (monocrystal areas) which are misoriented from one another.

X-ray diffraction analysis of 7F indicates that the sample consists of approximately equal quantities of α-In and In_2Bi, with no other crystalline phases detected.

3. Sample 8

The No. 8 samples contained copper coated tungsten spheres, argon gas and the In-Bi eutectic alloy. The objective of this demonstration was to achieve a uniform dispersion of the dense spheres and argon gas bubbles in an aligned lamellar eutectic matrix.

a. Radiographs

Figures 33 and 34 are radiographs at 0° and 90° of the control and flight capsules, respectively. The down direction for the control sample, and the heat sink position in both cases, is at the bottom of the picture. The control sample is in contact with the bottom and wall of the capsule. The indicated convex shape of the top surface is misleading. It is probably due to loose tungsten spheres--the true solid surface is more nearly flat (see below). The flight sample is in contact with the capsule only at isolated places. These patterns are consistent with the macrostructures observed for the two samples (see below).

b. Samples After Removal From the Capsule

Figures 35 through 37 are photographs of the samples after removal from the capsules. The dull surface, particularly, of the flight sample

is a result of being covered with tungsten spheres (unresolvable at this magnification). The control sample can be seen to have a reasonably flat top surface.

Figure 38 presents photographs of the No. 8 samples after the first longitudinal sections. The saw has obliterated most of the internal structural details.

c. Structural Observations

No. 8 Control

Figure 39 is the macrostructure of Section 8C-A-00. There are few tungsten spheres in the bulk of the control sample. There are a few trapped in the matrix of the last material to freeze at the end opposite the chill. The remainder of the spheres were not incorporated into the solidified sample and were found on the external surfaces (Figure 40). If any of the spheres were dispersed in the melt prior to solidification, they were pushed ahead by the liquid-solid interface because of their non-wetting characteristics or settled out under gravitation.

The macrostructure indicates that freezing did not occur in a planar interface normal to the axis of the sample. There even appears to be some independent nucleation at several points on the wall of the container. A number of In_2Bi dendrites can be seen in an area of the end opposite the chill (Figure 41). The most likely reason for these is the melt being off the eutectic composition.

No. 8 Flight

Figure 42 is a schematic of the sections which were taken of sample 8F-A. The macrostructure of Section 8F-A-00 is shown in Figure 39. A considerable number of the spheres are found within the sample, primarily in the shrinkage pores (Figures 43 and 44). As with the other flight Samples 4 and 7, solidification appears to have initiated at a number of sites, so that the pore and sphere distribution is macroscopically quite uniform throughout the sample.

This sample is unique among the No. 4, 7 and 8 samples in that the microstructure has large areas of aligned fine lamellar eutectic typical

of the classical directionally solidified eutectics (Figure 45). This is probably the result of alloy chemistry and solidification rate which occurred only in this sample. Several rosette growth structures can also be seen (Figure 46).

d. Chemistry

Qualitative emission spectrographic analysis of chips from Sample 8C-A indicated the presence of small amounts of W and Cu in the In-Bi matrix (Table 4). The low W and Cu contents support the lack of a great deal of entrapment of the spheres in the control sample.

e. X-ray

An X-ray diffraction scan of the 8F-A-00 surface indicated approximately equal quantities of α-In and In_2Bi. Tungsten was not detected because the principle tungsten peaks are masked by the matrix constituent peaks.

An X-ray Laue back reflection photograph indicated two or three areas of uniform orientation which are misoriented relative to one another.

C. LABORATORY EXPERIMENTS

A few experiments were performed in the laboratory to support or elucidate some of the observations made on the control and flight samples.

1. Microstructures

An attempt was made to duplicate the "Chinese script" structures which were observed in several of the samples. One of the main variables was believed to be the solidification rate. In-Bi alloy from a No. 7 spare capsule was melted in an alumina crucible. Small buttons of alloy were solidified by (1) chill casting into a cold copper mold, (2) air cooling the crucible and melt and (3) furnace cooling the crucible and melt. The samples were then examined metallographically. Aside from obvious differences in lamellae width, the structures were similar. There was no degenerate or script structure.

TABLE 4

QUALITATIVE EMISSION SPECTROGRAPHIC ANALYSIS
OF SAMPLE 8F-A-00

Element	Amount Present
In, Bi	10-100%
W	1000-10,000 ppm
Cu	100-1000 ppm
Al	10-100 ppm
Cr, Pb, Pd, Sn, Si, Tl	3-30 ppm
Ca, Fe, Ni	1-10 ppm
Ag, Mg	0.3-3 ppm
Mn	0.1-1 ppm

It was concluded that the solidification rate alone is not responsible for the script structure. Solute distribution and temperature gradient are, of course, additional factors which are undoubtedly important.

2. Macrostructures

The macrostructures in the majority of the samples suggested very little directionality in the solidification process. A sample was directionally solidified in a Pyrex tube at about 10 cm/hr by lowering it out of a furnace at 500°F into flowing cold water about an inch from the end of the furnace. The longitudinal section of the sample showed a great number of In_2Bi primary dendrites in the bottom third of the casting, longitudinally aligned. This sample, as was Sample 8C, was off eutectic composition. The upper part of the sample consisted of highly aligned (longitudinally) eutectic colonies. This degree of alignment was observed only in very small portions of Samples 4C and 7C. It appears that modifications should be made to the Apollo 14 experimental apparatus in order to improve the directionality of the composites.

3. Solidification Shrinkage

A number of observations which were made on the samples indicated that the In-Bi eutectic alloy shrinks on solidification. At the same time, there was some uncertainty among the various investigators of the Apollo 14 demonstration samples on this subject. An approximate value for the solidification shrinkage was obtained by directionally solidifying the eutectic in a graduated tube so that a reasonably planar interface resulted after completion of freezing. Measurement of this interface position in the liquid and in the solid just below the melting point yielded a shrinkage value of 2%. On a volume basis, this is 6%. However, because of the directional nature of the solidification, the true volume contraction on freezing is probably closer to 2% than 6%.

4. Thermal Conductivity

The eutectic appears to have a very low thermal conductivity, making it difficult to maintain a planar growth interface without the use of a moving heat source. Even in a Pyrex container, immersing its tip in cold

water resulted in a large pipe at the top after completion of solidification. This accentuates the need for experimental design to maintain unidirectional growth.

VI. CONCLUSIONS AND RECOMMENDATIONS

A. CONCLUSIONS

- Directional Solidification

Observations, particularly of the macrostructures, indicate that solidification in both the control and flight samples was not unidirectional. This problem can be solved by changes in the experimental design and procedure.

- Differences in Nucleation and Growth

Even without solidification directionality, interesting structural differences were observed between the flight and control samples. Some of these are related to the nature of the contact between the liquid and the capsule. In the flight samples, there was at best intermittent contact, resulting in unusual nucleation and growth structures (such as the rosettes). These results enhance the probable implications of the free-float sting experiments planned for Skylab, and suggest that very interesting solidification structures should result.

- Dispersion

While the non-wetting characteristics of the whiskers and spheres clouded the results somewhat, it is clearly evident that it is possible to produce dispersions of gases and dense phases in a melt which can be maintained during the solidification process only in reduced gravity.

B. RECOMMENDATIONS

The observations made on the Apollo 14 demonstration samples suggest several modifications or new approaches which might be taken in future experiments.

- Directional Solidification

There are several modifications that can be made to improve directionality of solidification.

Directionality will be improved by using a matrix of higher thermal conductivity, such as Al-33% Cu. However, from melting point considerations, the In-Bi eutectic may be the only logical choice.

The use of a low thermal conductivity material for the container walls, and high thermal conductivity material for the container bottom will improve directionality. The walls might be a glass, a ceramic, or stainless steel. The bottom could be aluminum, copper, or even silver. Any materials which are contemplated should be checked for compatibility with the matrix.

A two-stage resistance heater might be used, in which the top half is partially powered during solidification to assist in maintaining a temperature gradient during solidification. Additional capsule mass at the top to store heat could provide the same function.

- Dispersions

The advantages of reduced gravity in maintaining a dispersion during solidification would have been even more striking had the dispersants been wet by the melt. Such an experiment would be very interesting. A more sophisticated variation would include the use of two growth rates for a given dispersant size, faster and slower than the critical rate required for incorporation of a particle as measured in the terrestrial laboratory.

- Maintenance of Heat Flow

While the lack of contact of melt and container in the flight samples produced some very interesting results, it would also be useful to carry out experiments in reduced gravity in which contact is ensured. One approach might utilize spring mechanisms, as in the Skylab directional solidification apparatus.

APPENDIX A

PHASE I - SAMPLE SELECTION

A. INTRODUCTION

The initial phase of this contract consisted of a brief study of materials and fabrication techniques which could be used in the Composite Casting Demonstration. During this time, other contractors were considering metal matrix composites, immiscible liquid/solid systems of two or more components, and mixtures of gas and solid phase materials. NASA staff were also examining materials combinations as well as completing the details of the equipment and procedures to be used in the casting demonstration. Arthur D. Little, Inc., was assigned the study of inorganic and organic materials which might be used to simulate metal matrix composite preparation or directional solidification.

This study consisted of:

- initial screening of possible simulant materials
- laboratory tests to determine materials suitability
- preparation of procedures which could be used for the casting demonstration

As this work proceeded, the plans for the Apollo 14 casting demonstration were finalized. The materials we examined were not included in the final experiment configuration because of time pressures, uncompleted toxicity measurements, etc., and our efforts in this initial phase were discontinued in favor of examining the samples used in the flight program. This Appendix briefly documents some of this early work.

B. INITIAL MATERIALS SELECTION

We considered several types of materials as candidates for simulants of metal matrix composites: inorganic salt hydrates; salt eutectics; fluorocarbons; organic phosphates and silicates; and low melting organics. Fibers, whiskers and particles of metals, carbon, and inorganics were

considered for reinforcing materials. The principal criteria for selection of materials were:

- Melting point below 170°F
- Low toxicity
- Low flammability
- Low vapor pressure
- Readily available--flight approved materials
- Good simulant for crystalline metal matrix
- Transparent, if possible
- Significant density difference between matrix and reinforcing material
- Wetting of reinforcing material by matrix
- Chemical and physical compatibility of matrix material, reinforcing material and container

Astronaut safety was of prime importance

1. Inorganic Salt Hydrates

There are many congruent melting salt hydrates which have low melting points. A typical example is calcium nitrate tetrahydrate ($Ca(NO_3)_2 \cdot 4\ H_2O$). These materials are relatively inert, form defined crystalline structures, and are easy to work with. They present some difficulties for use because of vaporization of water and changes in stoichiometry and in the problems of nucleation--some inorganic hydrates supercool considerably and must be nucleated by seed crystals.

2. Salt Eutectics

There are over 60 halide eutectics which could also be used as materials for the composite experiment. These could be used for directional solidification either with or without fibrous materials. These experiments might simulate the directional solidification of the copper-aluminum alloy of the M-512 experiment. Directional solidification of

eutectics in zero-g may lead to unique structures because of the absence of convective effects. The principal difficulty with salt eutectics was thought to be the corrosiveness of the materials.

3. Fluorocarbons

Fluorocarbons generally include all organic compounds containing fluorine; however we restricted our attention to those containing only carbon, hydrogen and fluorine since these are the least flammable and least reactive chemically. Unfortunately, most of the fluorocarbons are liquids with melting points outside the range of interest to the program; however, several have melting points below 170°F. The principal problem expected of fluorocarbons is their potential toxicity.

4. Organic Phosphates and Silicates

Several organic phosphates and silicates have the appropriate melting range and form well defined crystalline structures. The principal problem with these materials are their potential toxicity and the difficulty in obtaining them in desired purity.

5. Low Melting Organics

A large number of organic compounds form transparent crystalline structures and have melting points in the proposed range of the composite casting experiment. An example of these is succinonitrile, which is a nitrogen derivative of succinic acid ($NCCH_2CH_2CN$). This material has been used by investigators in model studies of composites.[3] Succinonitrile is a crystalline organic with a sharp melting point of 54.5°C and thus can simulate metals which are also generally crystalline. The material has been used before in earth-bound modeling experiments. It is a transparent organic and can be observed because of strain induced color changes during the solidification process. While the flammability and toxicity need to be examined closely, the nitrogen substitution may result in decreased flammability over other organic compounds. Other crystalline organics have been used for modeling purposes and should be explored.

(3) British Ministry of Technology Establishments, Berks, England, New Scientist, 23 November 1967, p. 481.

6. Additives

Many metals can be obtained in whisker or fiber form and could be used as a reinforcing material. A wide range of densities could be achieved by using wires of beryllium, aluminum, steel or tungsten. Filaments of glass, boron, graphite or silicon carbide also are readily available, along with whiskers of silicon carbide, aluminum oxide or silicon nitride. Spheres of oxides (Al_2O_3, Zr_2O_3) and metals (Cu, W) could also be used. Because of this wide range of available materials of various densities, we devoted only limited attention to selection and examination of reinforcing materials.

7. Materials Selected

Table A-1 shows the principal materials examined and selected early in the program along with the potential problems expected of each material. From this screening we selected $Co(NO_3)_2$, tri-p-tolylphosphate, decafluorobiphenyl and benzophenone for laboratory screening tests.

C. LABORATORY SCREENING TESTS

A series of simple laboratory tests were conducted to determine the crystallization behavior--nucleation rate, and apparent strength--materials compatibility, flammability, and wetting characteristics of the materials shown below:

Material	MP	Characteristics
$Co(NO_3)_2 \cdot 6\ H_2O$	135°F	Readily available laboratory reagent, red monoclinic crystals
Tri-p-tolylphosphate	169-170°F	Eastman Kodak No. 1483
Decafluorobiphenyl	155°F	Aldrich Chemical, D-22-7
Benzophenone	120°F	Readily available laboratory reagent, rhombic crystals

1. Crystallization Behavior

The crystallization behavior was observed by melting and recystallizing samples in glass vials and aluminum tubes as follows:

TABLE A-1

PRINCIPAL MATERIALS SCREENED AND SELECTED FOR LABORATORY TESTS

	Potential Problems
1. Inorganic Salts and Hydrates	
$Ca(NO_3)_2$	Supercooling problems, requires nucleation
$Co(NO_3)_2$	Checkout in Lab
$MnCl_2$	Compatibility of chlorides with container
$Na_2S_2O_3$	Low melting point (120°F)
$Ni(NO_3)_2$	Checkout in Lab; if $Co(NO_3)_2$ is not found suitable
NaAc	Recrystallization problems may occur
2. Inorganic Eutectics	
Over 60 Chlorine Salt Eutectics including:	Compatibility problems and potential toxicity
$GaCl_3$ - CuCl	
KCl - $SbCl_3$	
$GaCl_3$ - NaCl	
$GaCl_3$ - $CdCl_3$	
$HgCl_2$ - $SbCl_3$	
$AgNO_3$-Tl NO_3	Toxicity
3. Fluorocarbons	
Decafluorobiphenyl	Checkout in Lab
Octafluoronaphthalene	Checkout in Lab if decafluorobiphenyl unsuitable
4,4'-Dihydrooctafluorobiphenyl	Flammability
2 Fluorobiphenyl	Flammability
2 Fluoronaphthalene	Flammability
Undecafluorocyclohexane	Low melting point

TABLE A-1 - Continued

	Potential Problems
4. Organic Phosphates and Silicates	
Tri-p-tolylphosphate	Checkout in Lab
Tri-phenylphosphate	Low melting point
Tetra-p-tolylsilicate	Questionable availability
5. Organics	
Acelaldoxine	Low melting point
Acetamide	N_2 compounds on decomposition, toxicity
Acetoacetanilide	N_2 compounds on decomposition, toxicity
Acetylferrocene	Toxicity
m-acetylphenylbenzoate	Low melting point
6-amino-1-hexanol	Flammability
Benzophenone	Checkout in Lab
Butadiene Sulfane	Flammability, toxicity
Succinonitrile	Toxicity

Glass Vial Tests

Use 3 1/2 gm each material in glass vials, flush with nitrogen, seal with screw caps

Place in room temperature water, heat slowly, remove when melted

Cool in insulating styrofoam block (a) with directional heat transfer

Observe crystallization rate and nucleation

Aluminum Tube Tests

Use 5 gm each material in Al tube, flush with N_2, seal with glass slide and silicone grease

Place in room temperature water, heat slowly and remove when melted

Cool in (c) insulating styrofoam block; (d) desk top; (e) ice water (total immersion); (f) ice water (partial immersion)

Observe crystallization rate and nucleation

The results of these tests are given below:

Crystallization Rate		Melt Time (min)	Crystallization Time (min)					
			a	b	c	d	e	f
1	$Co(NO_3)_2$	5-6	19	20	24	13	2	2
2	Tri-p-tolylphosphate	7	--	5	16	10	1.5	2
3	Decafluorobiphenyl	3-4	--	2	10	12	1	1
4	Benzophenone	5-6	28	> 60	> 60	> 60	> 60	> 60

Conditions

(a) Glass container in styrofoam insulation
(b) Repeat of (a)
(c) Aluminum container in styrofoam
(d) Aluminum container on desk
(e) Aluminum container immersed in ice water
(f) Aluminum container with bottom in ice water

Nucleation

(1)	$Co(NO_3)_2$	Spontaneous
(2)	Tri-p-tolylphosphate	Spontaneous
(3)	Decafluorobiphenyl	Spontaneous
(4)	Benzophenone	Does not nucleate by itself, Fresh copper and glass nucleate, Tungsten does not

These results indicated that benzophenone was probably not suitable because of the uncontrollable nucleation rates. Relative strength of the materials was observed by inserting sharp objects into the crystallized substances. $Co(NO_3)_2$ was the least strong; some liquid was present in several samples. The other materials seemed strong enough to be removed without much difficulty.

2. Materials Compatibility

Materials compatibility was determined by examination of containers and wire inserts after repeated contact with the four sample materials. The results indicated no specific compatibility problems with aluminum, stainless steel, or most reinforcing additives. We found that tri-p-tolylphosphate may discolor aluminum and thus be indicative of possible chemical reaction.

3. Flammability

Simple flammability tests were conducted by heating samples with an open gas flame. We found that cobalt nitrate was not flammable in air; tri-p-tolylphosphate burned in air under prolonged heating but was self-extinguishing in air; decafluorobiphenyl burned and smoked in air under prolonged heating but was self-extinguishing; and benzophenone burned in air. Samples of these materials were submitted to NASA for evaluation.

4. Wetting

We examined the wetting characteristics of each sample material with copper, aluminum, tungsten, boron and Teflon by inserting cleaned

fibers into molten samples and observing the meniscus formed at the interface. We obtained the following results:

$Co(NO_3)_2$	Wets	W,	Cu,	B?,	Al,	Not	Teflon
Tri-p-tolylphosphate	"	"	"	B	"	"	"
Decafluorobiphenyl	"	"	"	"	"	"	"
Benzophenone	"	"	"	"	"	"	"

5. Toxicity

We did not test samples for their toxicity. However, on the basis of handbook data and the chemical formulation of the materials, we estimated the following order of toxicity for the samples:

$Co(NO_3)_2$	Least
Benzophenone	
Decafluorobiphenyl	
Tri-p-tolylphosphate	Most

6. Overall Acceptability

On the basis of these test results, we concluded that cobalt nitrate was the most acceptable material and that decafluorobiphenyl was next most promising. The final choice of samples would have to await detailed toxicity and flammability tests.

D. SAMPLE PREPARATION AND EXAMINATION PROCEDURES

During the first phase of the program, we prepared procedures for preparing and examining samples for the Apollo 14 experiment. Some of these procedures were discarded because the materials were not included in the final sample selection. Other procedures were modified and changed as the experiment evolved. Tables A-2 and A-3 are representative of the procedures developed.

TABLE A-2

EXPERIMENT NO. 11 -- FIBERS IN SIMULATED METAL MATRIX

Objective: To prepare a fiber composite in zero-g using a transparent (or translucent) crystalline matrix which simulates a metal matrix.

Significance: An easily visualized 3 dimensional distribution and alignment of fibers in a matrix of significantly different density.

Procedure for Performing Experiment (Astronaut)

a. Heat (standard time)

b. Remove and shake (standard shake)

c. Directionally cool (standard time)

Procedure for Preparation of Experiment

a. Components -- decafluorobiphenyl, cobalt nitrate or sodium acetate crystals

-- uncoated (or coated) boron fibers (100 mil long)

-- tungsten mixer--to be determined based on other experiments

b. Composition -- 12 volume % fibers

c. Specimen Procedures:

Boron fibers:	clean with organic solvents and distilled water; dry
Crystals:	recrystallize three times
Mixture:	melt crystals, mix in fibers, pour into flight container, continue agitation until solidified (at MSFC)
Seal:	seal tubes (using "O" ring and EB weld)

d. Specimen Quantity for 12% volume fiber, 20% argon

Argon	- 3.25 cm^3
Boron Fibers	- 5.0 g
Decafluorobiphenyl	- 19.6 g
or Cobalt Nitrate	- 20.8 g
or Sodium Acetate	- 15.5 g

TABLE A-2 - Continued

Evaluation Procedure for Returned Sample

1. Visual
2. Photographic (macro and micro)
3. Electron microscopy
4. Mechanical tests (compression, shear)
5. Others as appropriate

Miscellaneous

Removal of Sample From Container

Cut off both ends of sample container; push out with plunger

Alternates:
a. machine off aluminum
b. dissolve (with biphenyl)
c. cool sample, use heat pulse to melt outer layer and extrude with plunger

Notes:

1. Aluminum Oxide or Boron Filaments - Coating not required. Fibers and whiskers should be clean.

2. Decafluorobiphenyl - Do not recrystallize since this may introduce impurities. Melt in clean sealed glass tubes, purged with argon. Use controlled oil bath for melting. Filter using clean 50-60 mesh stainless steel screen only if molten material not clear.

3. Cobalt Nitrate - Recrystallization not necessary. Melt in clean sealed glass tubes, purged with argon. Use controlled oil bath for melting, make sure water is not vaporized during melting or adsorbed by molten material--use a tightly sealed system. Transfer quickly and seal rapidly to avoid loss or gain of water.

4. Sodium Acetate - Follow TRW established procedures, note that paraffin is not one of the components used, but may be used as a sealer. Transfer and sealing should be done rapidly to avoid loss or gain of water.

TABLE A-3

PRELIMINARY EVALUATION PROGRAM -- APOLLO 14
METAL COMPOSITES CASTING DEMONSTRATION

Experiment No. 2, 4, 5, 7, 8, 10 and 13

Preliminary recommendations for handling and analysis of post-flight and control samples are:

I. SPECIMEN HANDLING

A. Prior to evaluation -- For the metal matrix composites, the only important restriction after the experiment has been performed, both in the laboratory and post-flight, is temperature control. The upper end of permissible temperature is the remelt temperature. Rapid changes of temperature (e.g., dunking in sea water) at the low end should be avoided because of possible cracking of brittle constituents and interfaces.

II. EVALUATION PRIOR TO REMOVAL OF SPECIMENT FROM CAPSULE

A. Bulk radiography to determine filling of the capsule by the casting.

III. REMOVAL OF CASTING FROM CAPSULE

A. Machine off end cap, using sufficient coolant, and remove the casting. If the casting cannot easily be removed, then alternatives B and C will be employed, either individually or in combination.

B. Machine off the capsule, using sufficient coolant.

C. Chemically remove the capsule in a sodium hydroxide solution.

IV. POST REMOVAL EVALUATION

A. Measure bulk density of the casting to provide one measure of the volume percent gas content.

B. Examine the exterior surface of the casting to provide detail of shape, surface morphology, presence of voids, spheres, and fibers. Record photographically any such features.

C. Perform point source stereoradiography to determine the distribution of fibers, spheres, and pores in each casting. This will help identify those areas from which mechanical and metallographic samples should be taken. Predetermined sectioning schemes run the danger of missing important features, particularly if there are inhomogeneities in the casting.

TABLE A-3 - Continued

D. Sectioning of the casting to obtain samples for mechanical property tests will require a diamond wire saw for the samples containing spheres, fibers, and whiskers. An acid string saw can also be used to section the metal-gas samples.

E. Metallograph Specimen Preparation

   a. Mounting - Castable plastics should be used. Mechanical mounting can be used where the plastics are inappropriate.

   b. Surface preparation - Mechanical or chemical polishing should be used, but there are difficulties with composite materials. Abrasive blast equipment can also be used to develop surface topography. In certain cases, argon ion etching should be used as this will both etch and develop topography.

F. Microscopy - Optical microscopy can be employed to determine the general structural details. Interference microscopy can be used to study surface topography. The scanning electron microscope and replica electron microscopy can be used if the optical observation indicates a need for higher resolution.

G. Mechanical Tests

   a. Micro and macro hardness tests can be performed on the metallographic samples.

   b. A tensile test can be performed on a portion of each casting, provided the point source stereoradiography indicates a sufficient amount of material which is macroscopically homogeneous. Otherwise, a bend test can be performed, using a sample 0.1 x 0.2 x 3/4 in. The fracture surface will be examined in the scanning electron microscope.

H. Electron Microprobe - This technique can be used if there are any indications of reaction between the matrix and the spheres, fibers, and whiskers. This is unlikely at the low temperatures involved. The technique can also be used if the distribution of the matrix constituents cannot be resolved by the other microscopy techniques.

I. Additional Alternative Tests

   a. Gas analysis - to measure the volume and composition of the gas. This can be accomplished by carefully machining the end cap, removing gas with hypodermic tubing, and analyzing with mass spectrometry or gas chromatography.

TABLE A-3 - Continued

b. Sonic measurements - velocity and attenuation on intact samples or sections of samples.

J. Comparison of Test Results - All tests' results should be compared to control samples prepared under laboratory (1g) conditions.

FIGURES

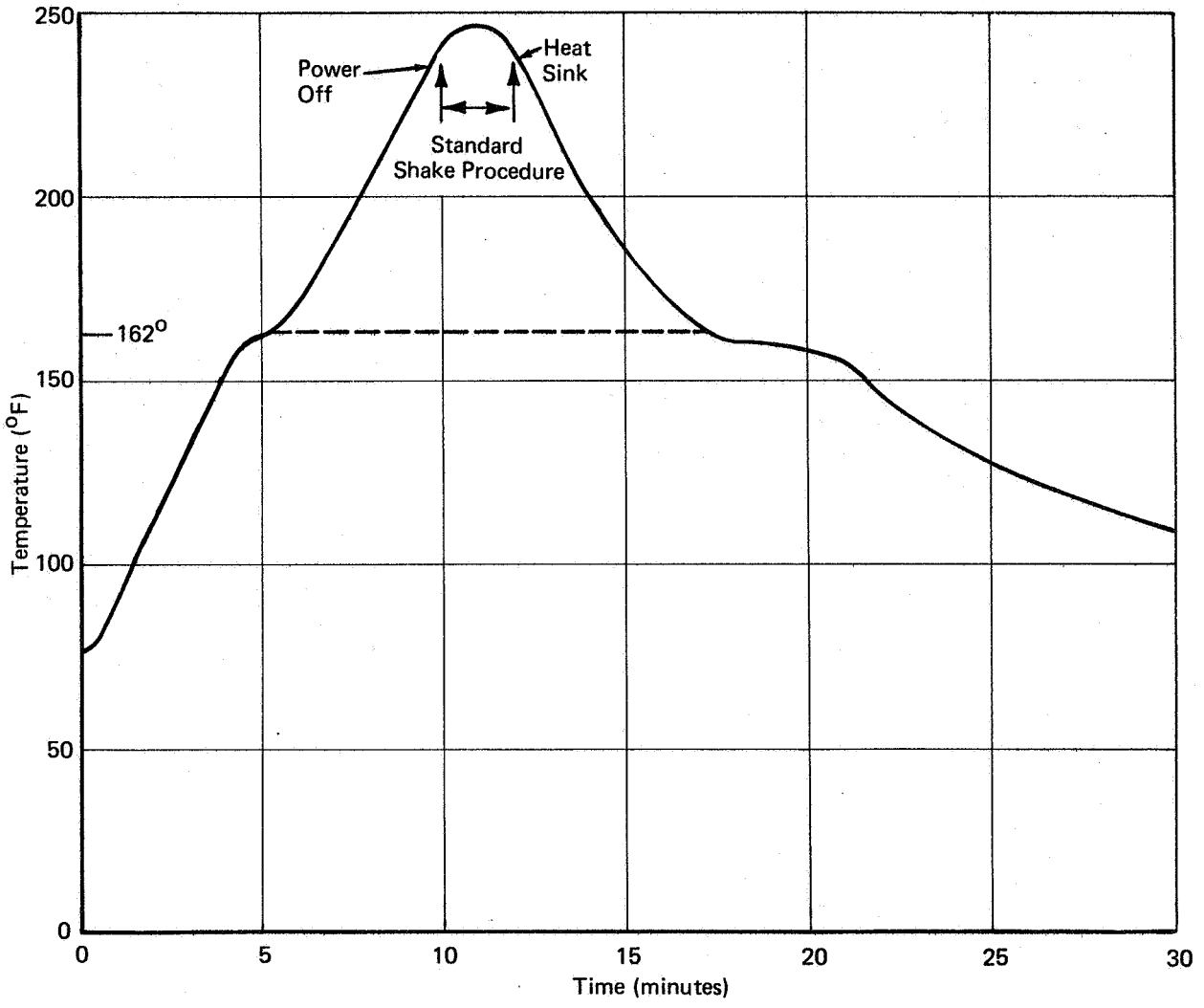

FIGURE 1 REPRESENTATIVE TEMPERATURE – TIME PROCESSING CYCLE FOR APOLLO 14 DEMONSTRATION SAMPLES

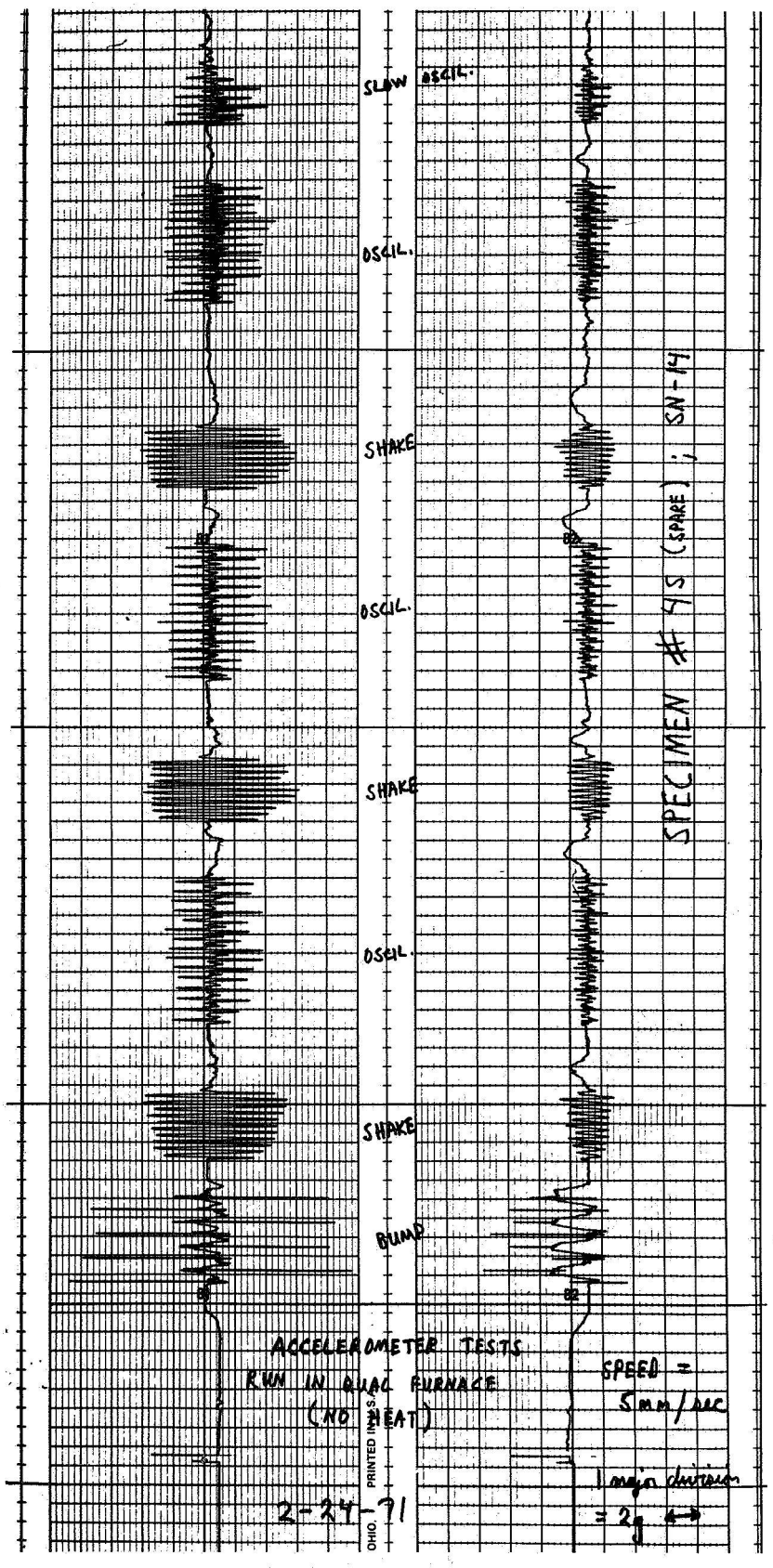

FIGURE 2 ACCELEROMETER MEASUREMENTS OF SIMULATED PROCESSING CYCLE FOR APOLLO 14 DEMONSTRATION SAMPLES

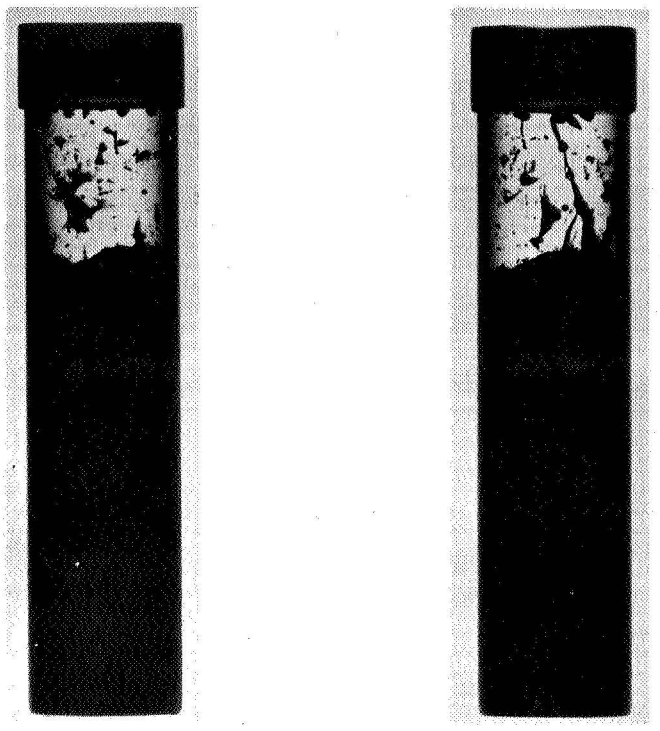

0° 90°

FIGURE 3 X–RAY RADIOGRAPHS OF SAMPLE 4C

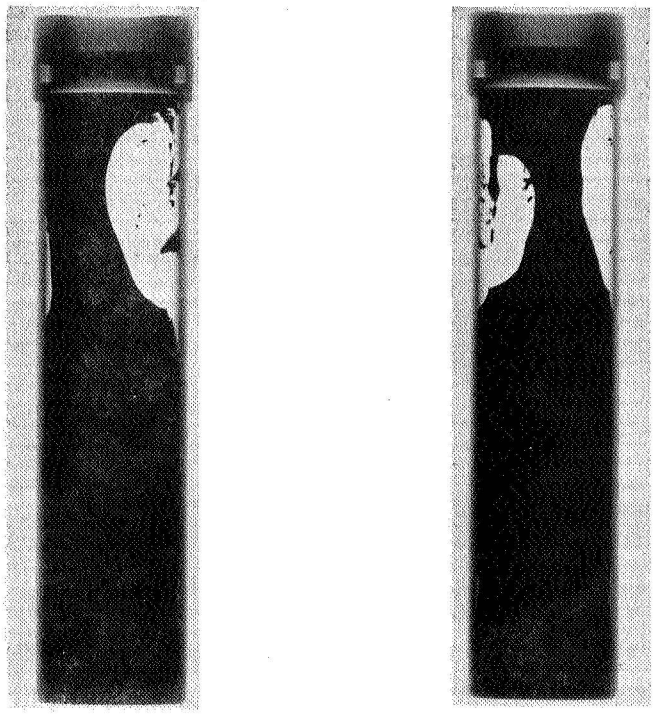

0° 90°

FIGURE 4 X–RAY RADIOGRAPHS OF SAMPLE 4F

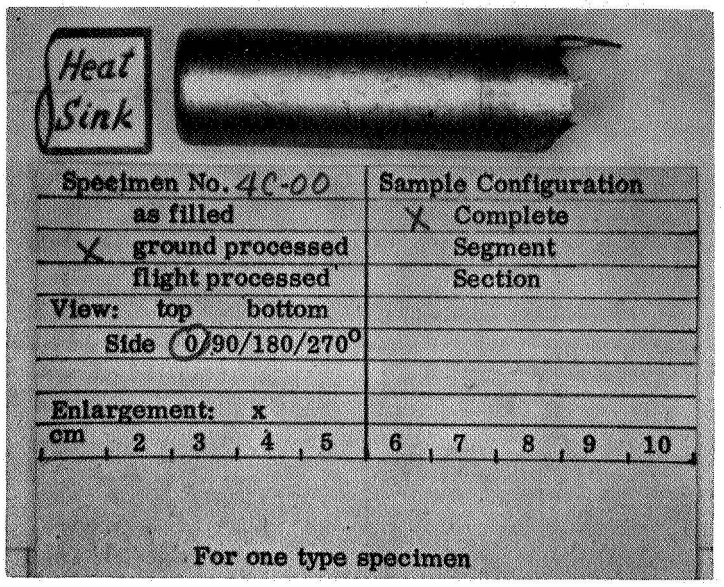

a.

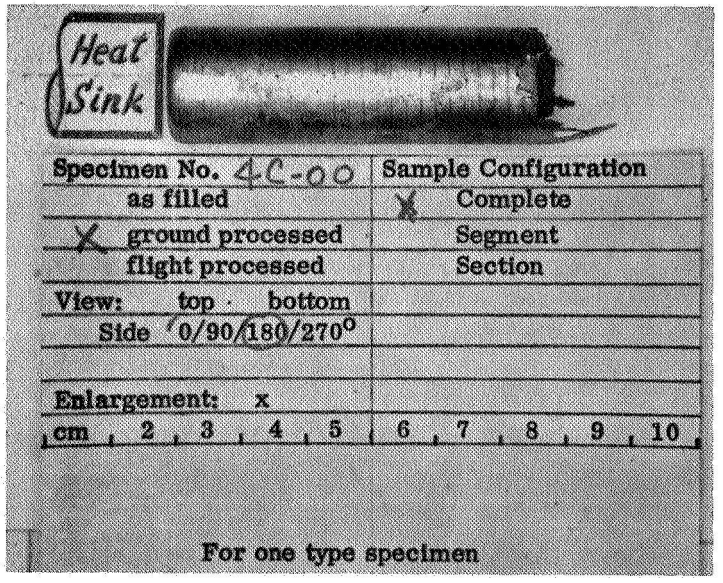

b.

FIGURE 5 SIDE VIEWS OF SAMPLE NO. 4C-00 AFTER REMOVAL FROM CAPSULE

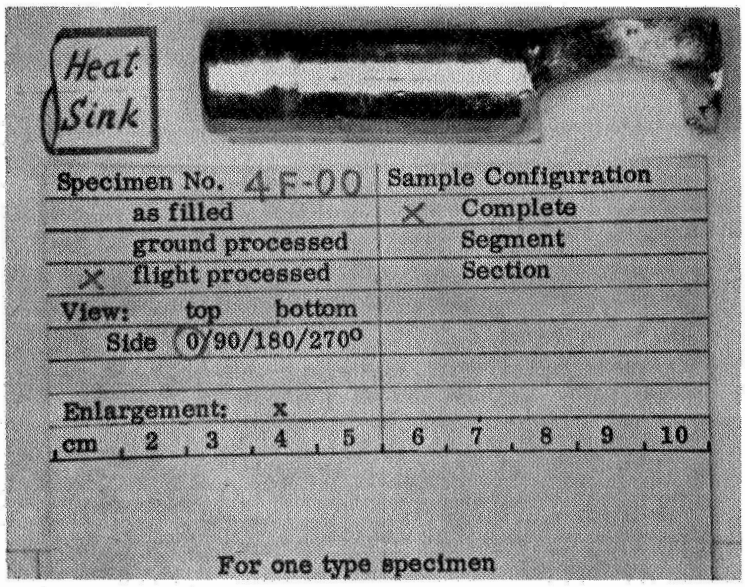

a.

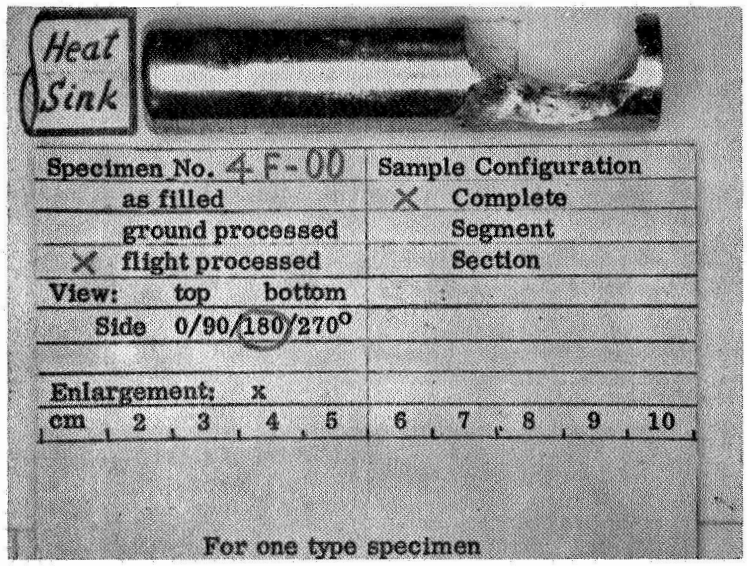

b.

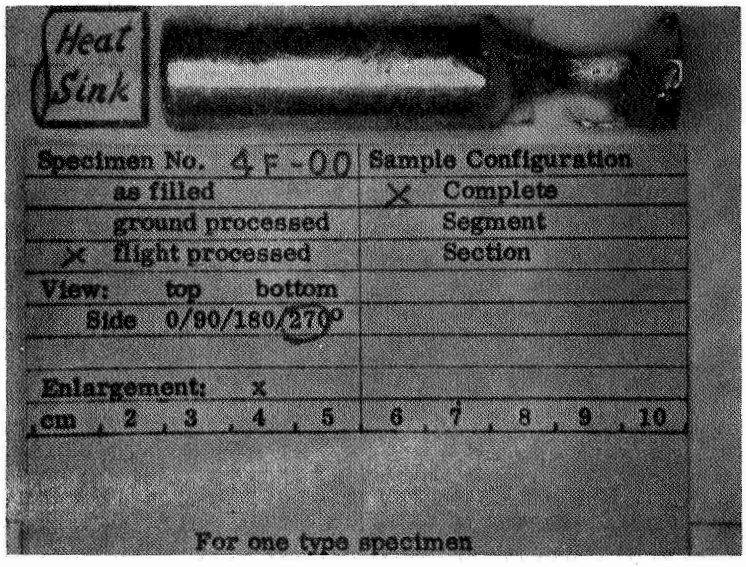

c.

FIGURE 6 SIDE VIEWS OF SAMPLE NO. 4F-00 AFTER REMOVAL FROM CAPSULE

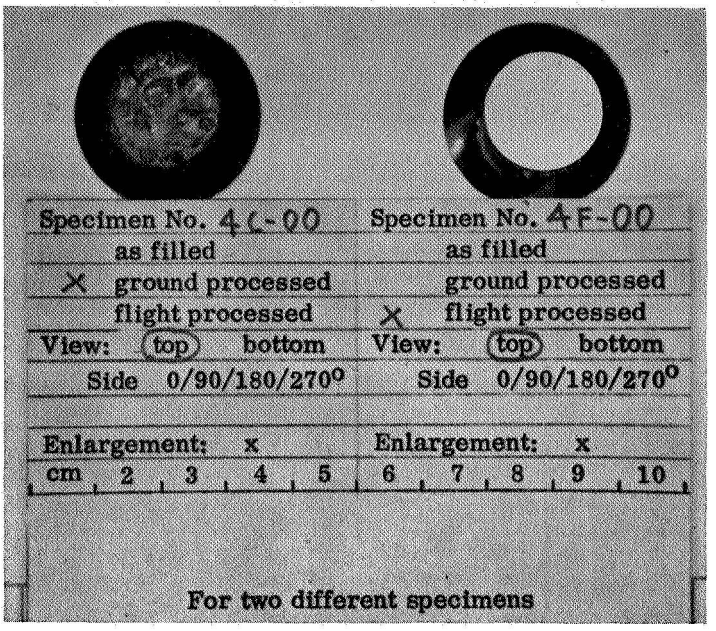

a.

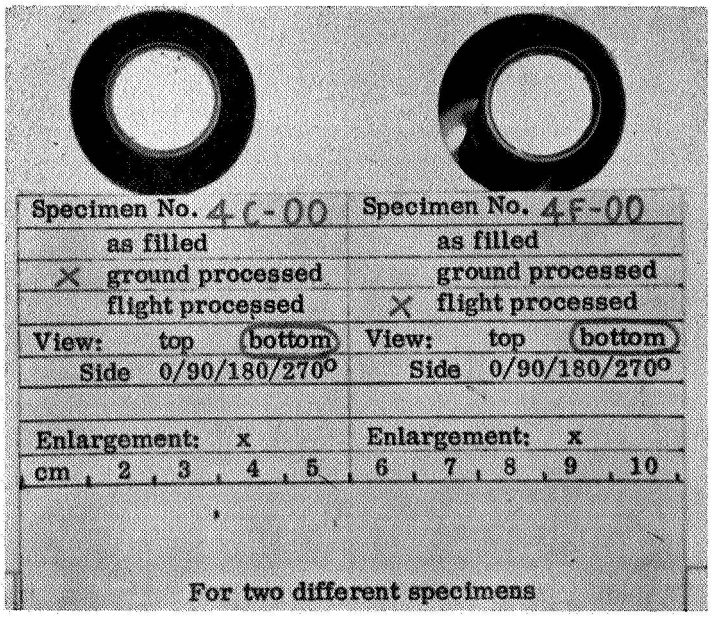

b.

FIGURE 7 END VIEWS OF SAMPLES 4C-00 AND 4F-00 AFTER REMOVAL FROM CAPSULE

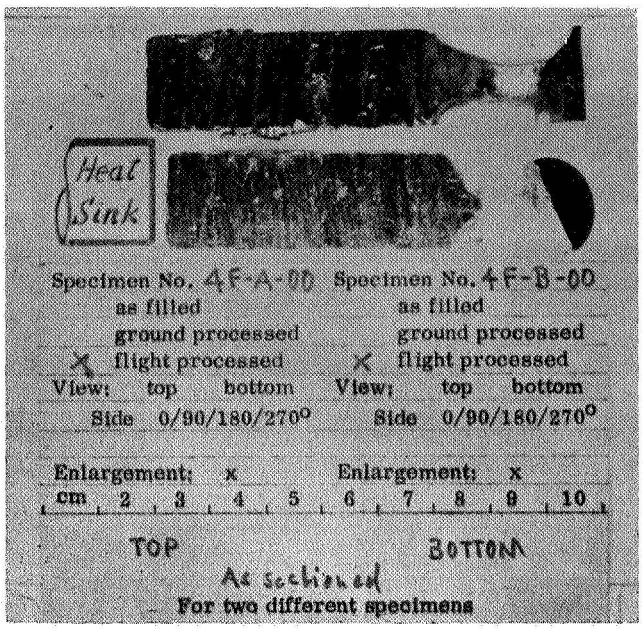

a.

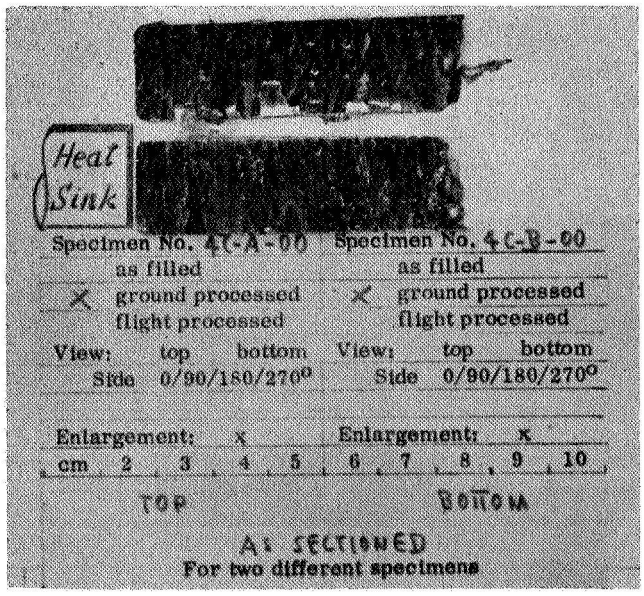

b.

FIGURE 8 PHOTOGRAPHS OF LONGITUDINAL SECTIONS OF SAMPLES 4C-00 AND 4F-00

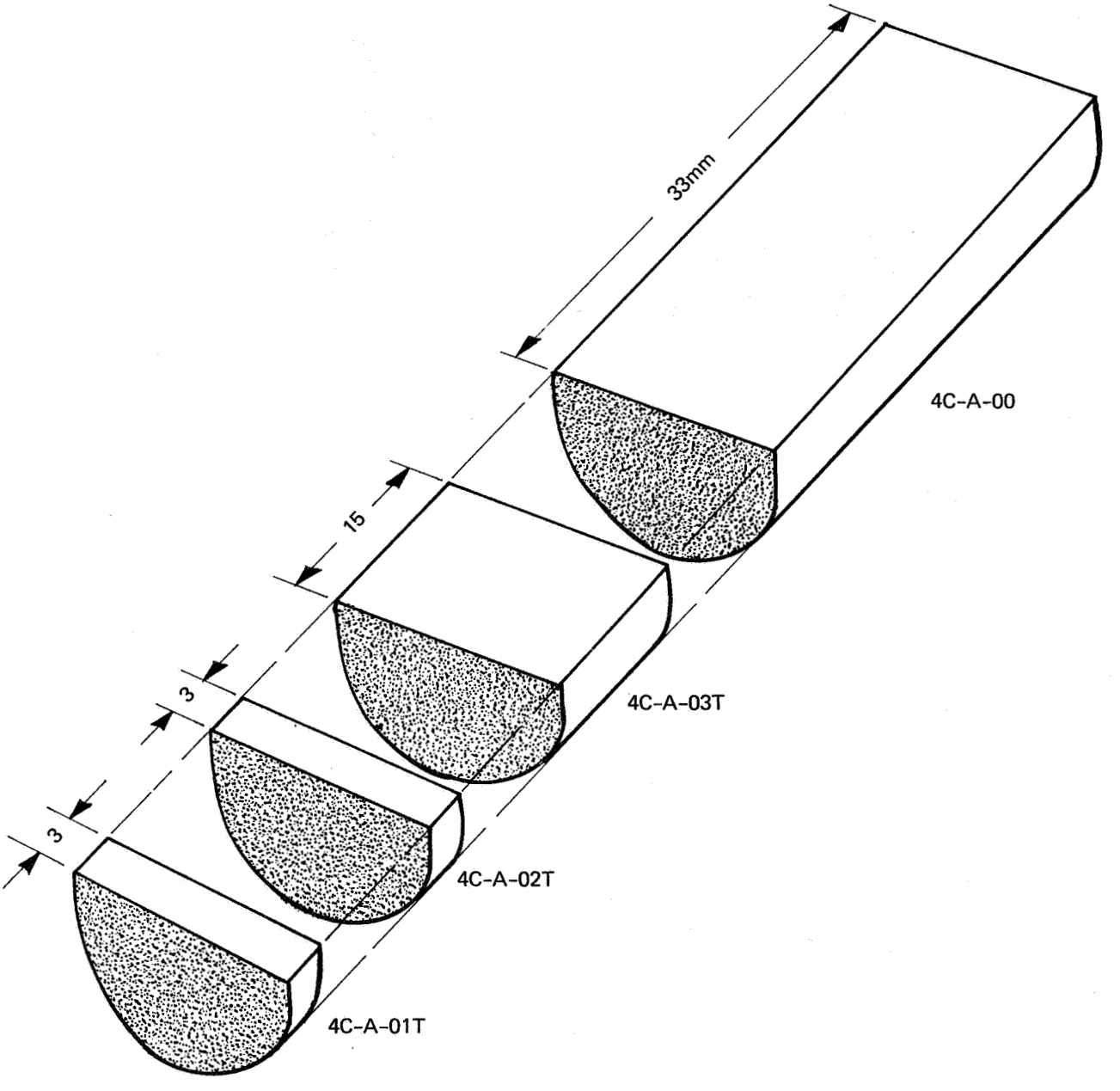

FIGURE 9 SCHEMATIC SKETCH OF SAMPLE SECTIONS FROM 4C-A-00

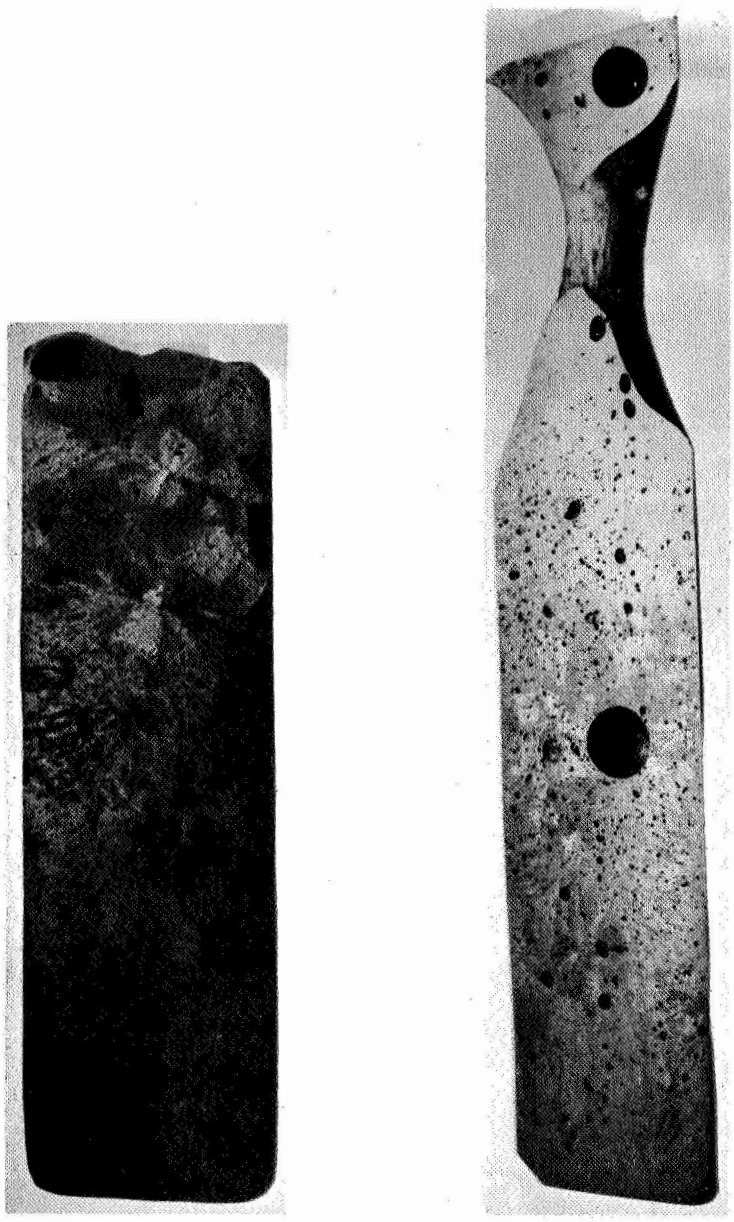

4C-A-00 4F-A-00

(Heat Sink End)

FIGURE 10 MACROPHOTOGRAPHS OF LONGITUDINAL SECTIONS, SAMPLES NO. 4C AND 4F, ETCHED, 2x

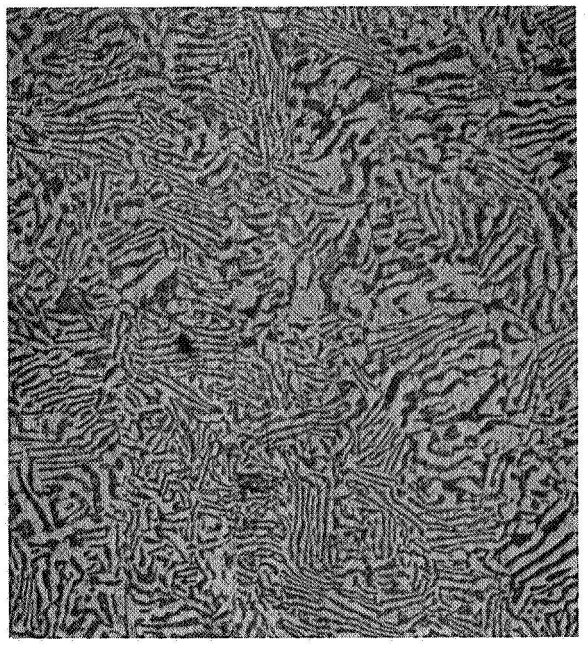

Adjacent to Capsule 125x

Center of Dense Zone 125x

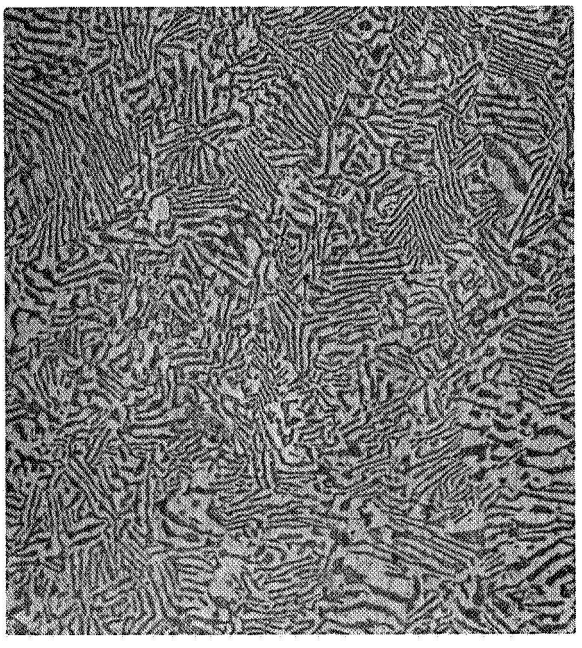

Top of Dense Zone 125x

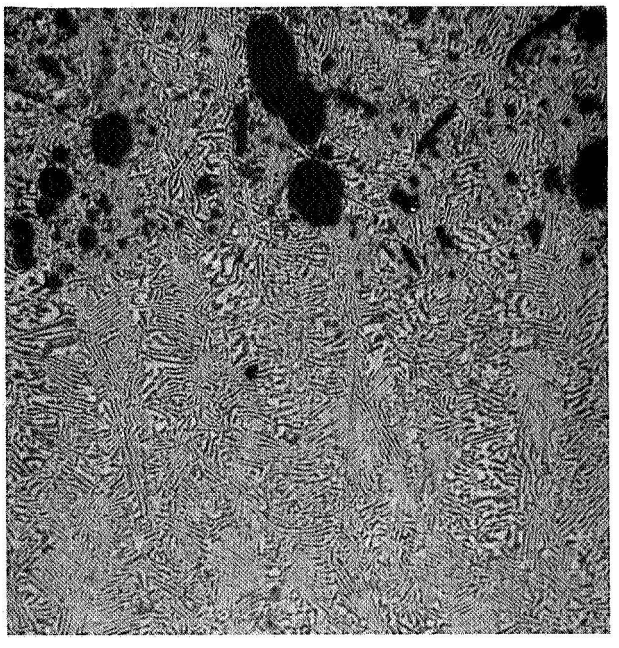

Dense – Porous Zone Interface 65x

FIGURE 11 STRUCTURE WITHIN THE FULLY DENSE REGION OF SAMPLE 4C-A-00 ETCHED (The Heat Sink is at the Bottom of the Page)

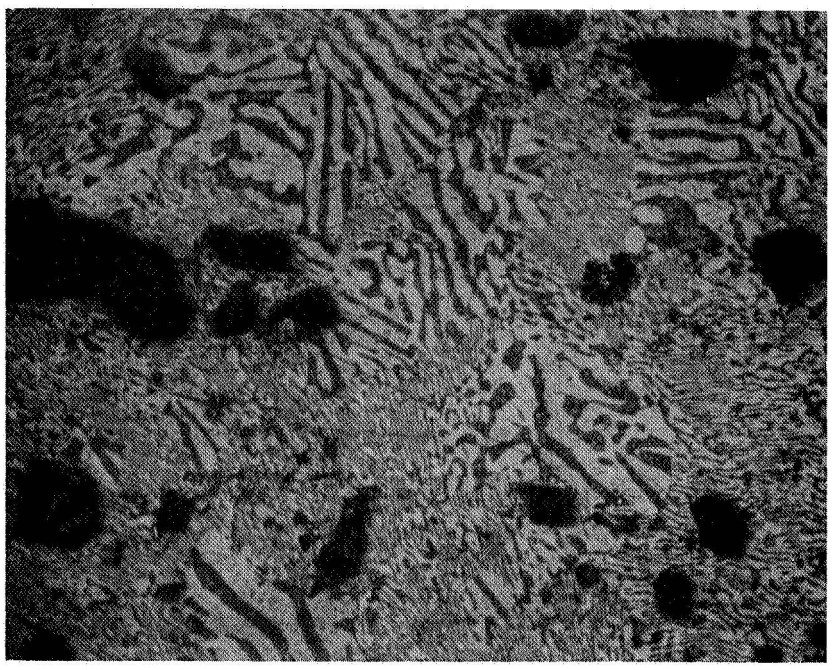

a. 250x

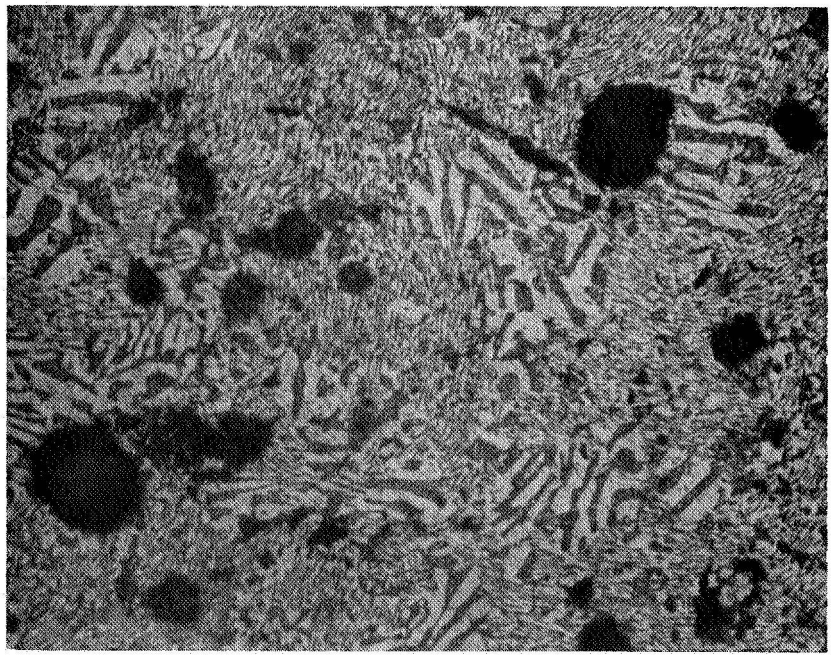

b. 250x

FIGURE 12 TYPICAL STRUCTURE WITHIN THE POROUS REGION OF SAMPLE 4C-A-00, ETCHED

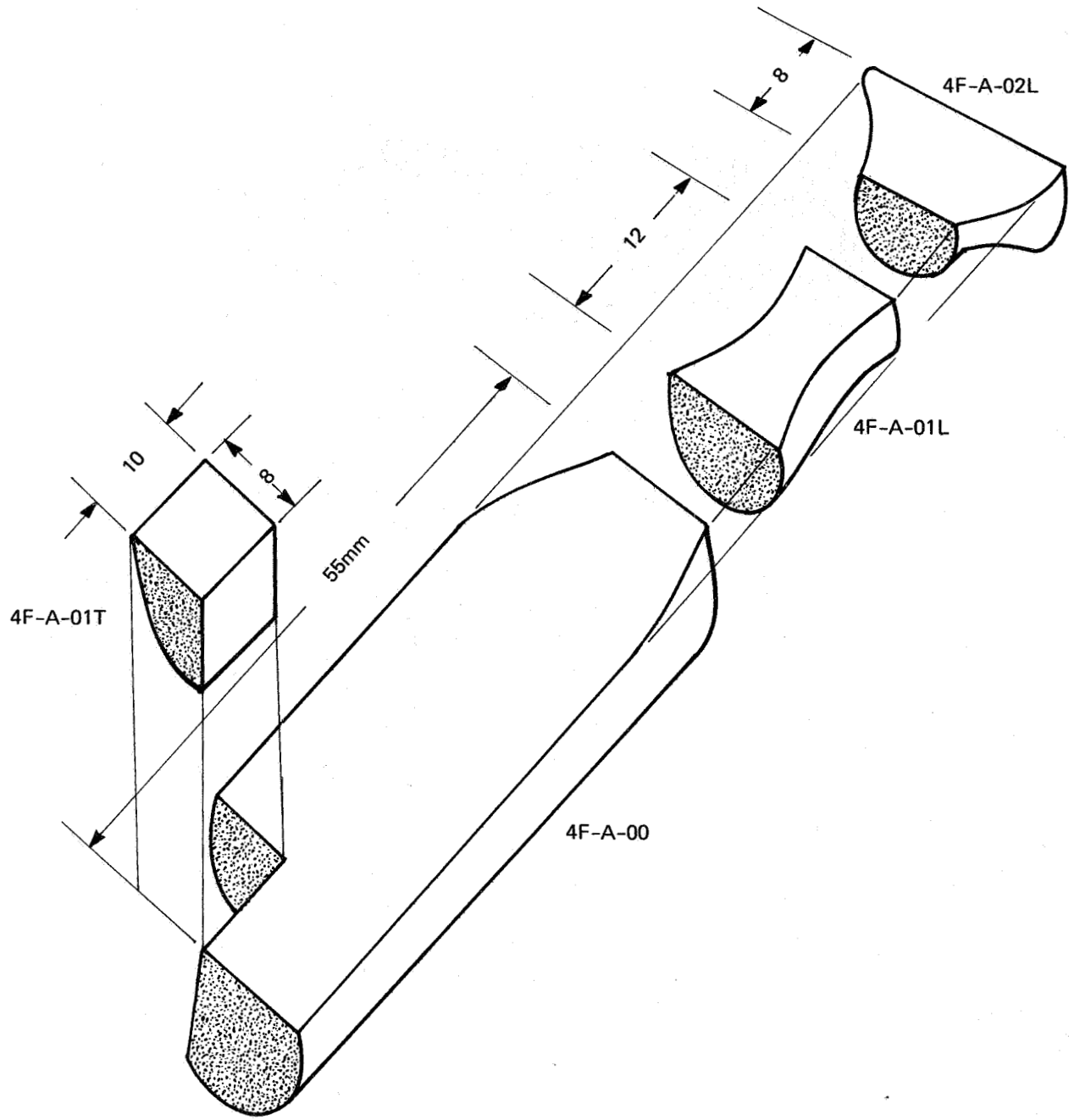

FIGURE 13 SCHEMATIC SKETCH OF SAMPLE SECTIONS FROM 4F-A-00

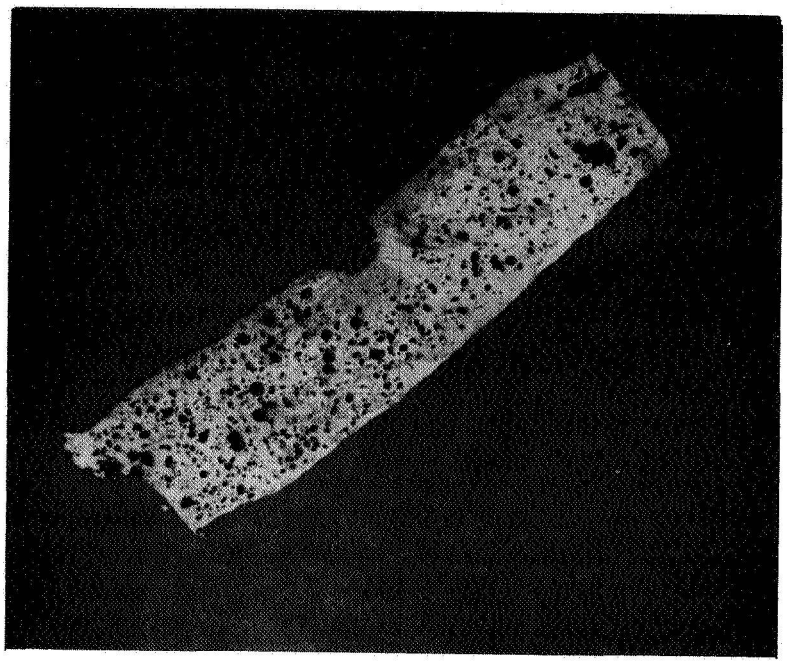

8x

FIGURE 14 LONGITUDINAL SECTION THROUGH NECKED PORTION OF SPECIMEN, SHOWING CONTINUITY OF STRUCTURE (Heat Sink End is toward Lower Left)

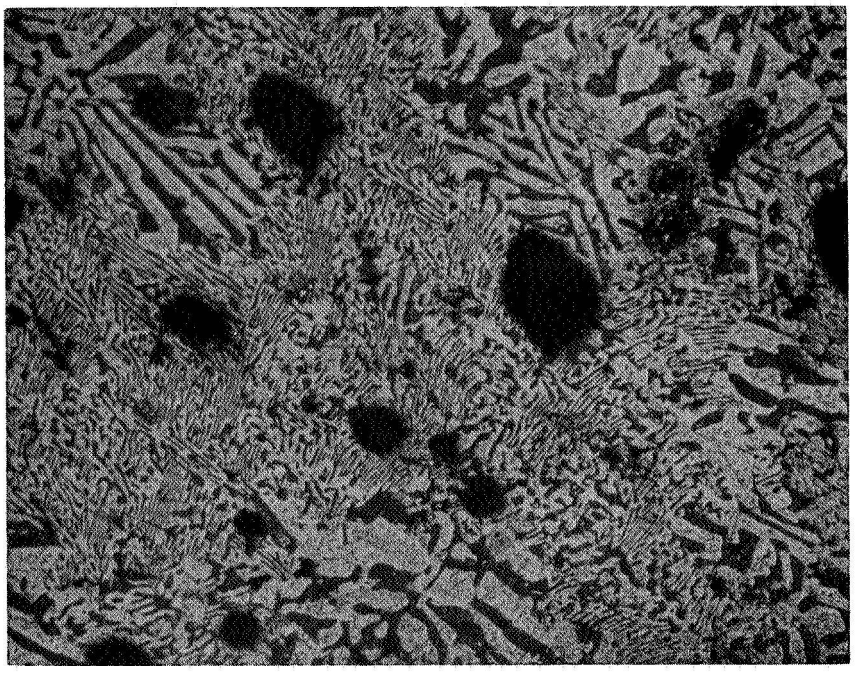

a. 250x

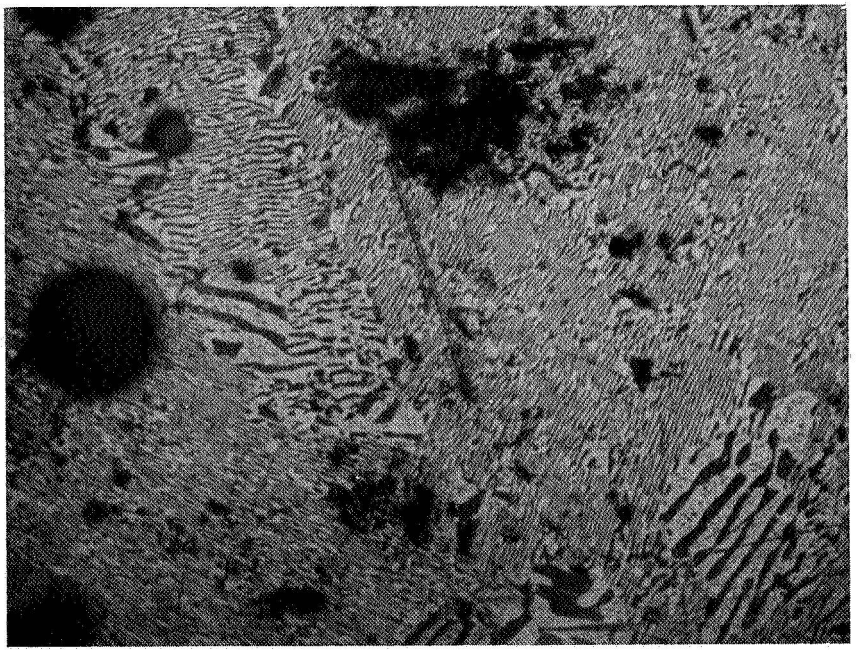

b. 250x

FIGURE 15 TYPICAL STRUCTURES WITHIN SAMPLE 4F-A-00, ETCHED
(Note SiC Fiber in Center of Lower Picture)

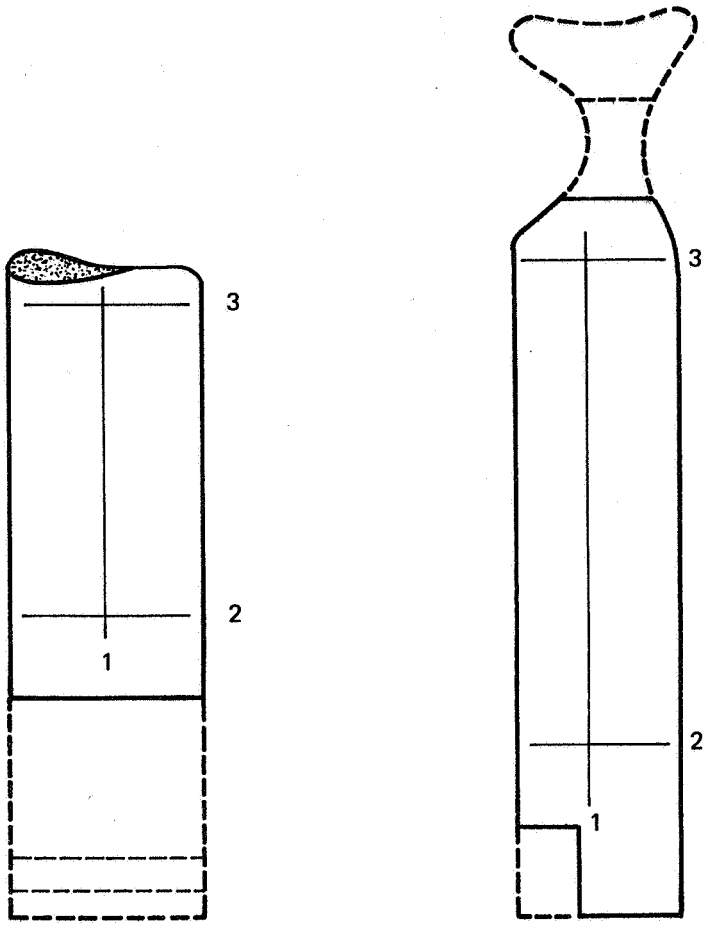

4C-A-00 4F-A-00

Pore Density

Average (1, 2, and 3)	8%	16%
Top (3)	5	19
Bottom (2)	13	16

Pore Size

Average	60μm	60μm
Median	43	37

FIGURE 16 DISTRIBUTION OF POROSITY IN NO. 4 SAMPLES

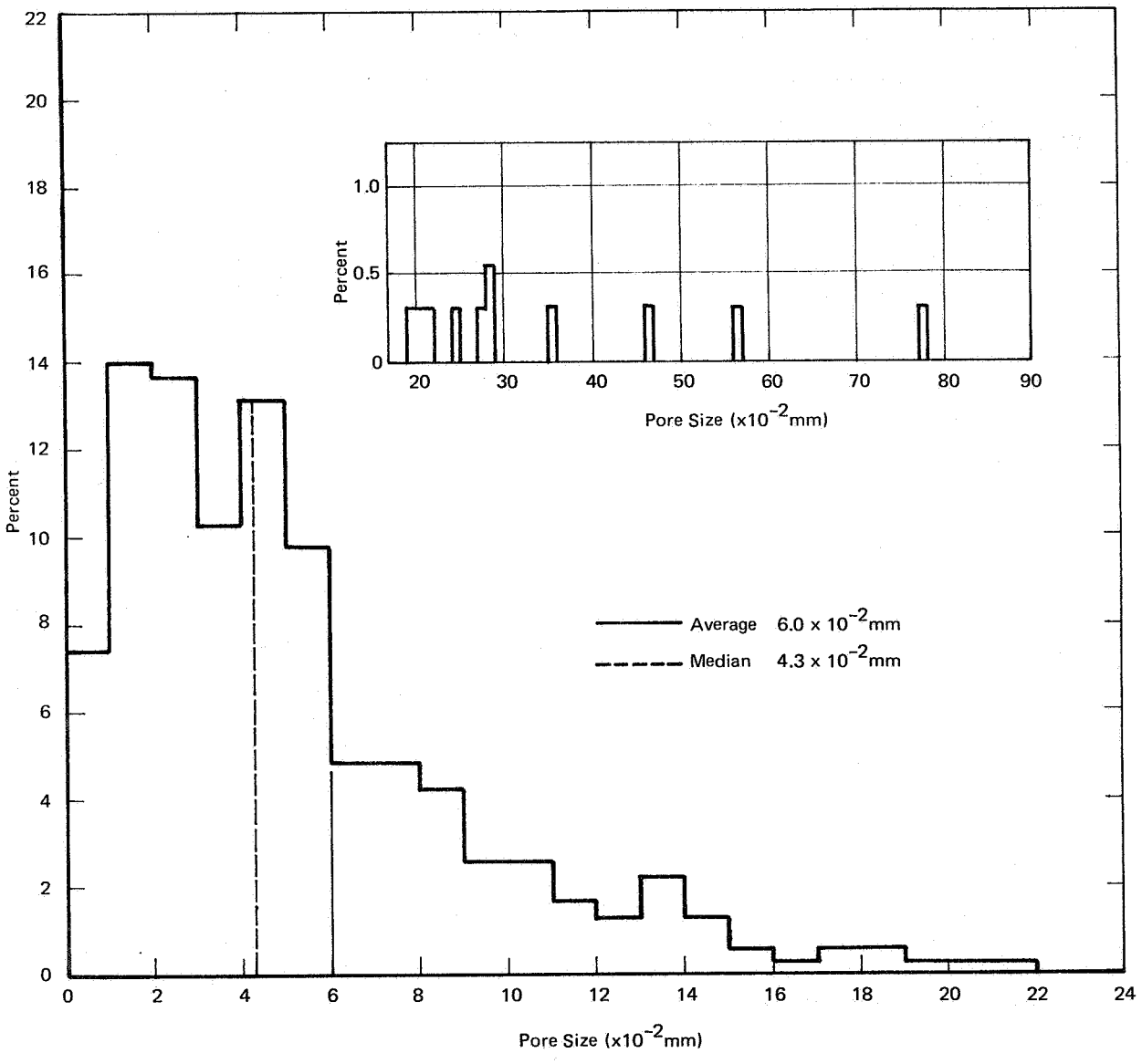

FIGURE 17 PORE SIZE DISTRIBUTION FOR SAMPLE 4C-A-00

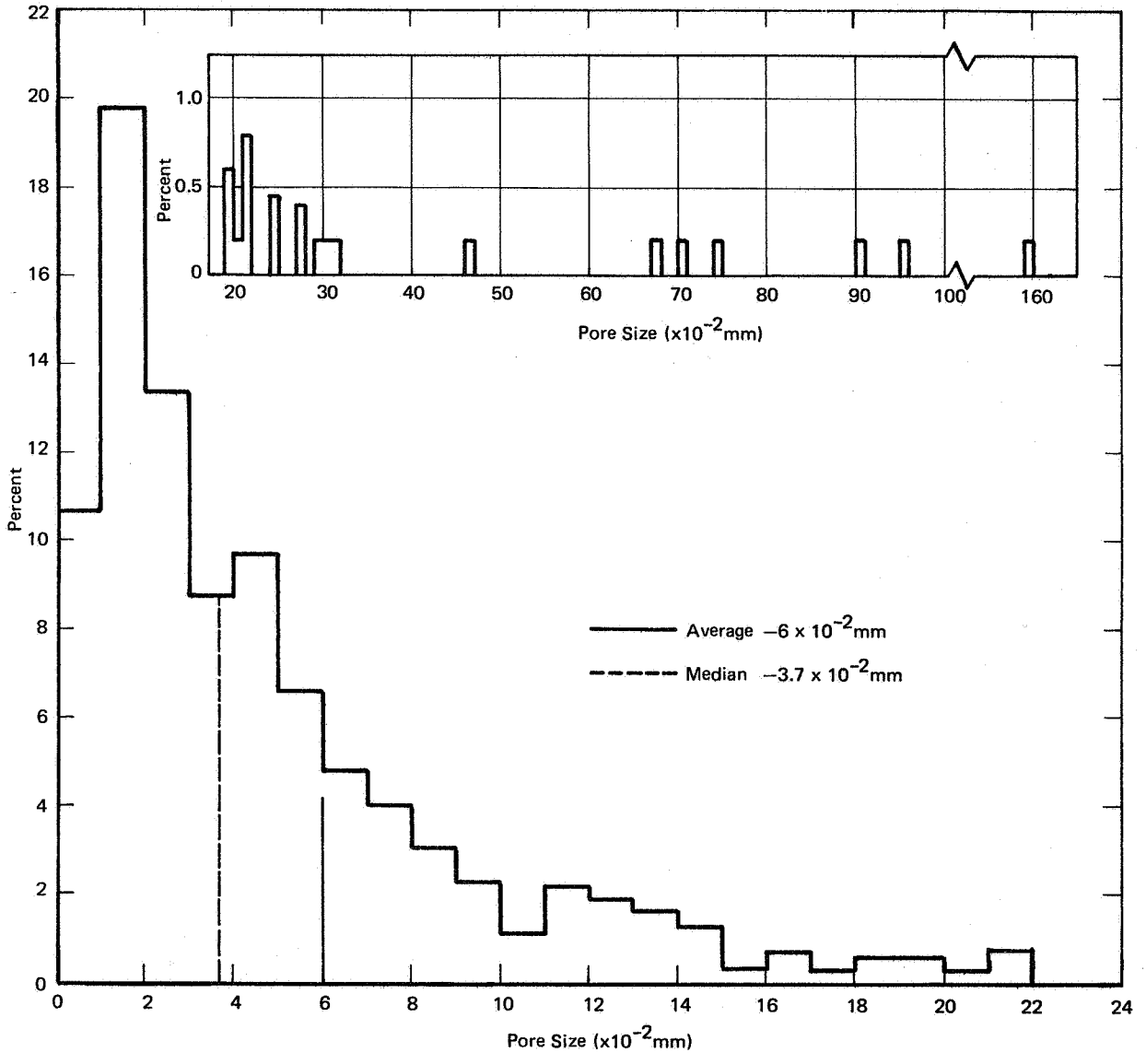

FIGURE 18 PORE SIZE DISTRIBUTION FOR SAMPLE 4F-A-00

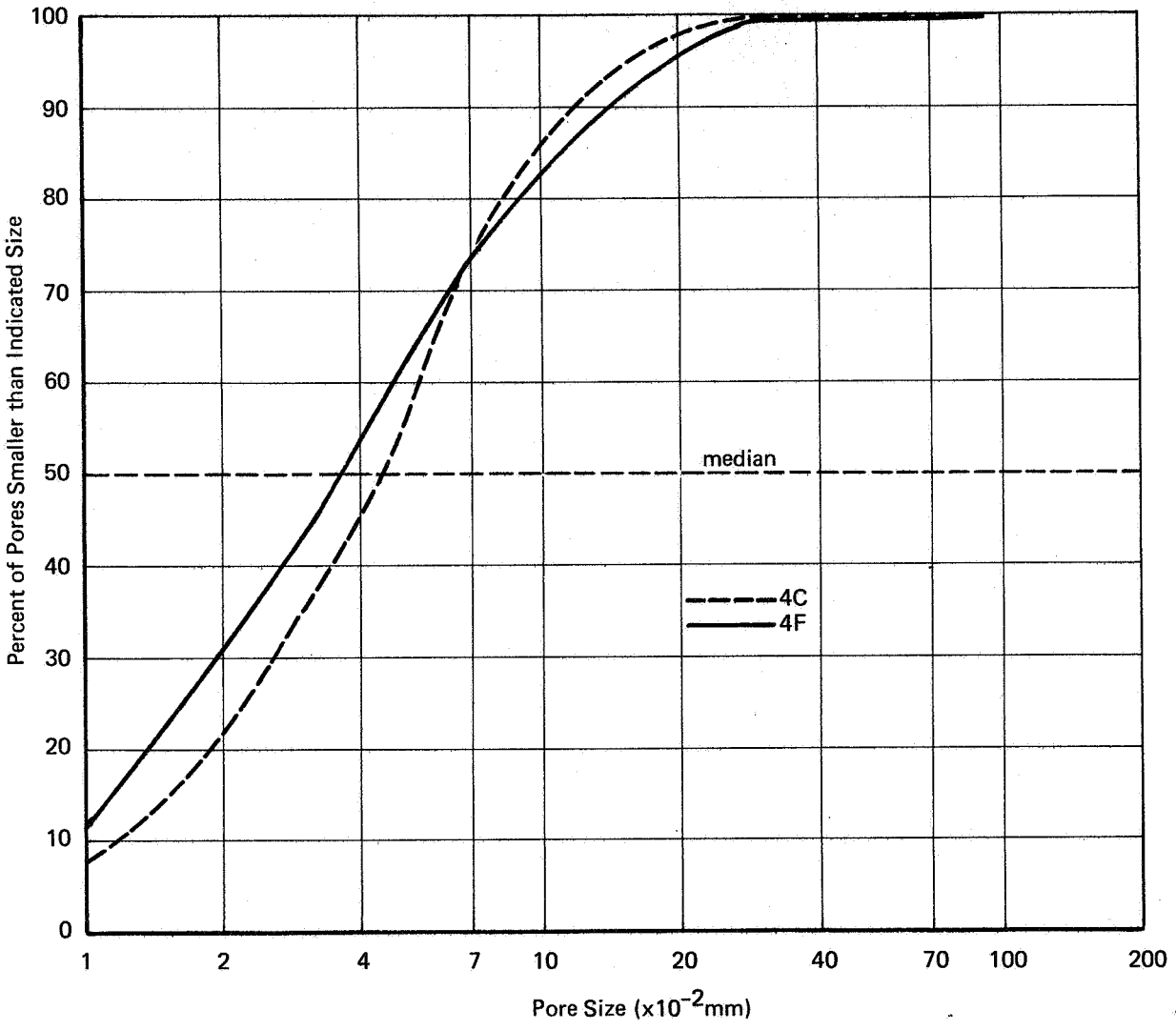

FIGURE 19 COMPARISON OF PORE SIZE DISTRIBUTION BETWEEN SAMPLES 4C-A-00 AND 4F-A-00

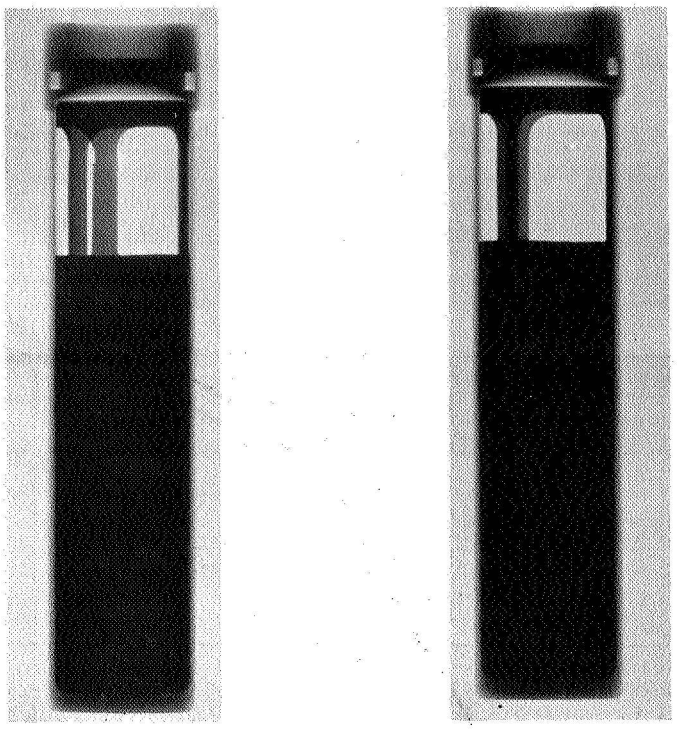

0° 90°

FIGURE 20 X–RAY RADIOGRAPHS OF SAMPLE 7C

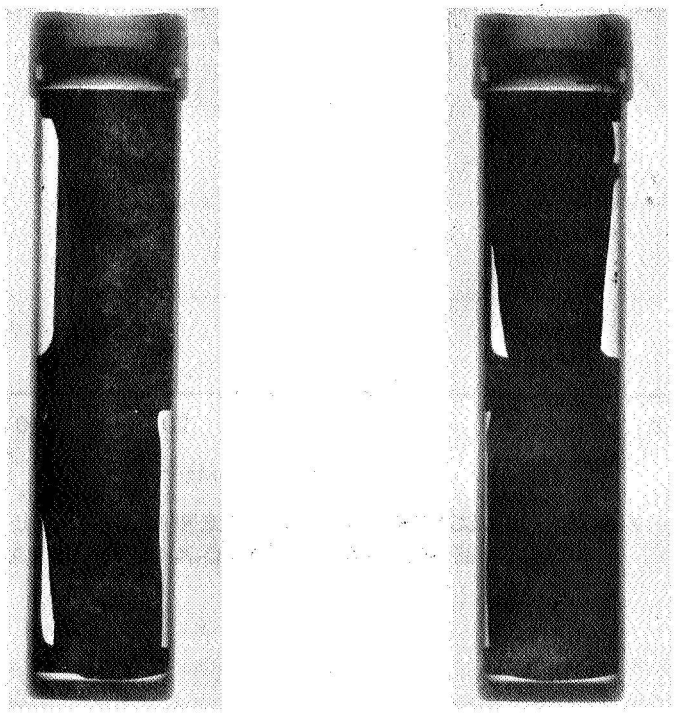

0° 90°

FIGURE 21 X–RAY RADIOGRAPHS OF SAMPLE 7F

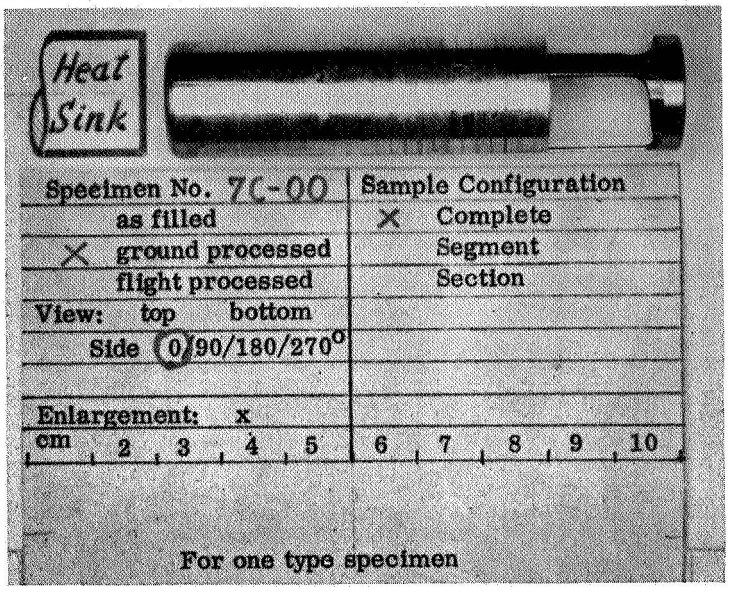

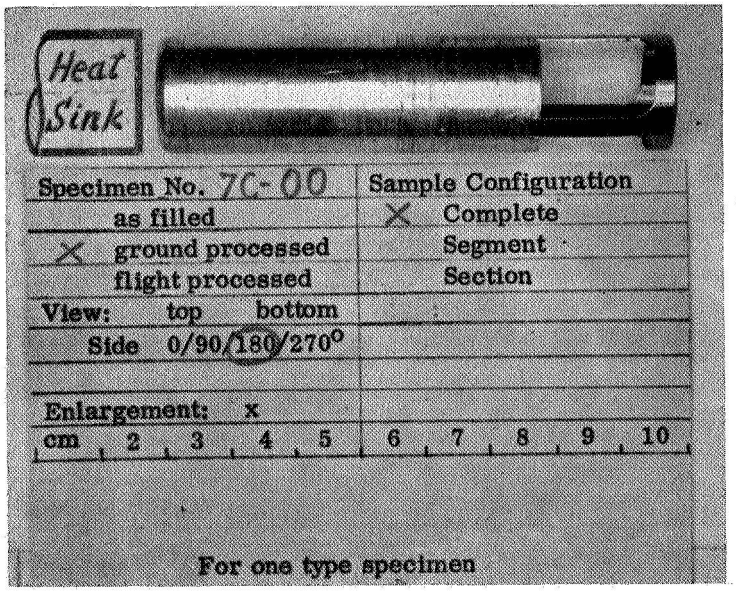

FIGURE 22 SIDE VIEWS OF SAMPLE NO. 7C-00 AFTER REMOVAL FROM CAPSULE

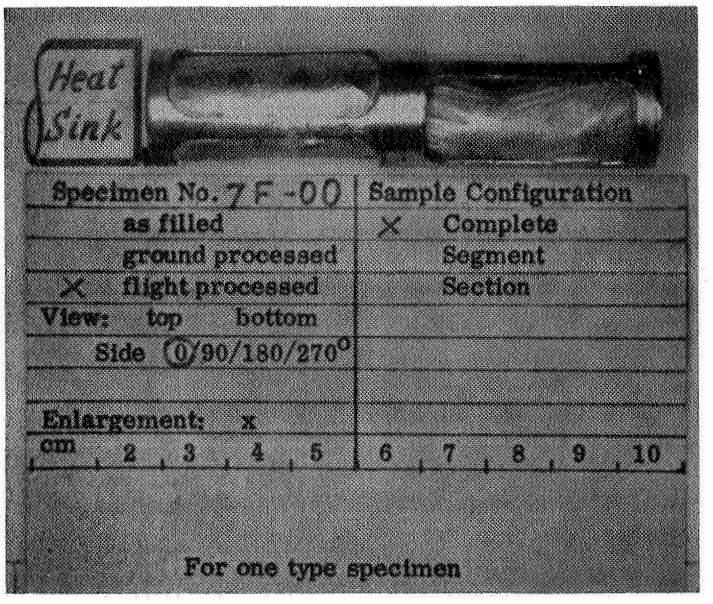

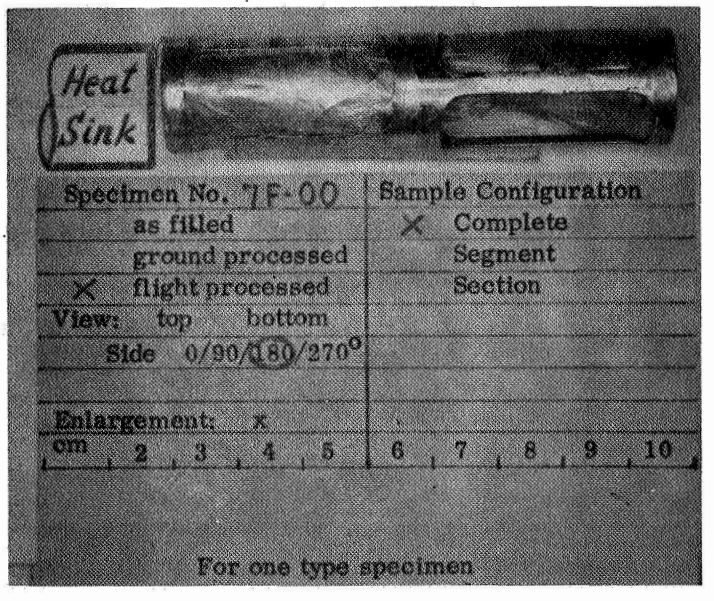

FIGURE 23 SIDE VIEWS OF SAMPLE NO. 7F-00 AFTER REMOVAL FROM CAPSULE

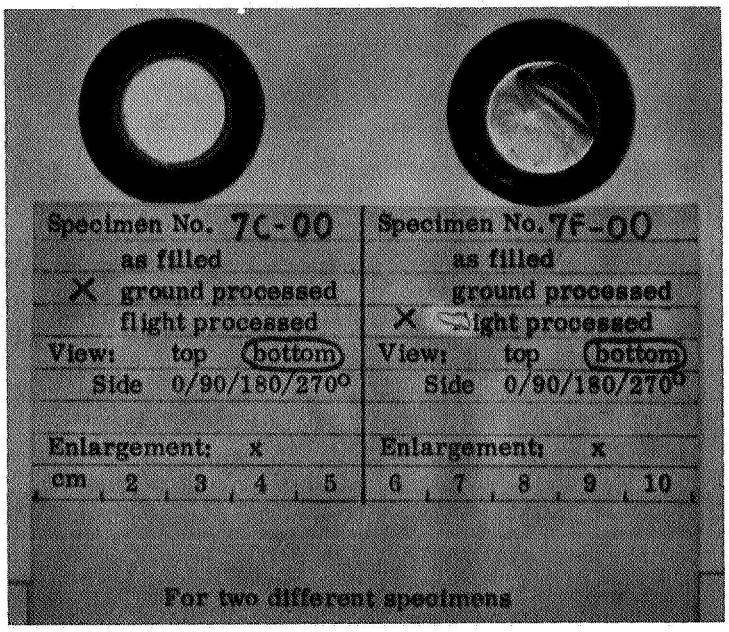

FIGURE 24 END VIEW OF SAMPLES NO. 7C-00 AND 7F-00 AFTER REMOVAL FROM CAPSULE

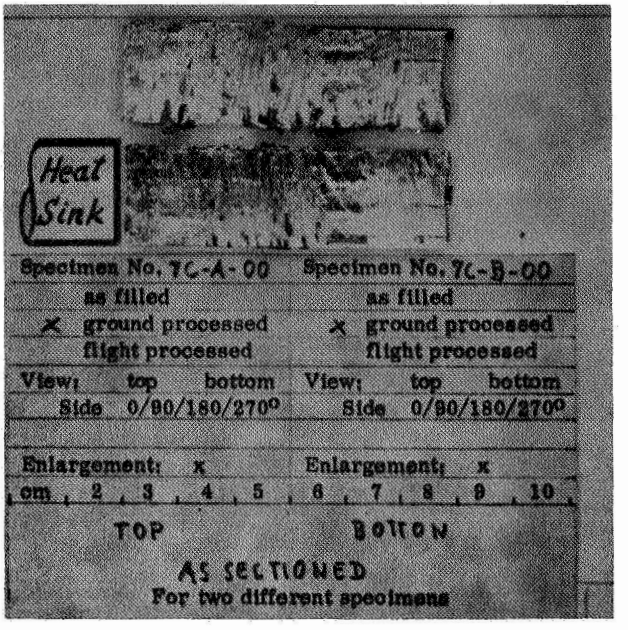

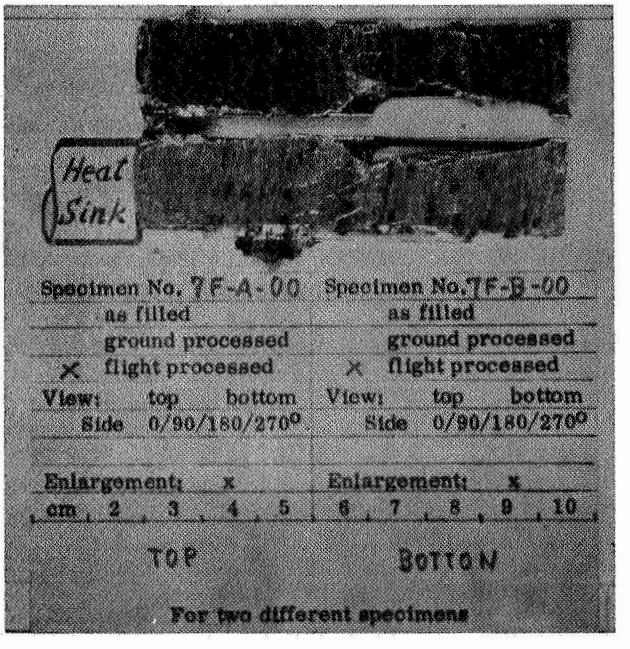

FIGURE 25 PHOTOGRAPHS OF LONGITUDINAL SECTIONS OF SAMPLES 7C-00 AND 7F-00

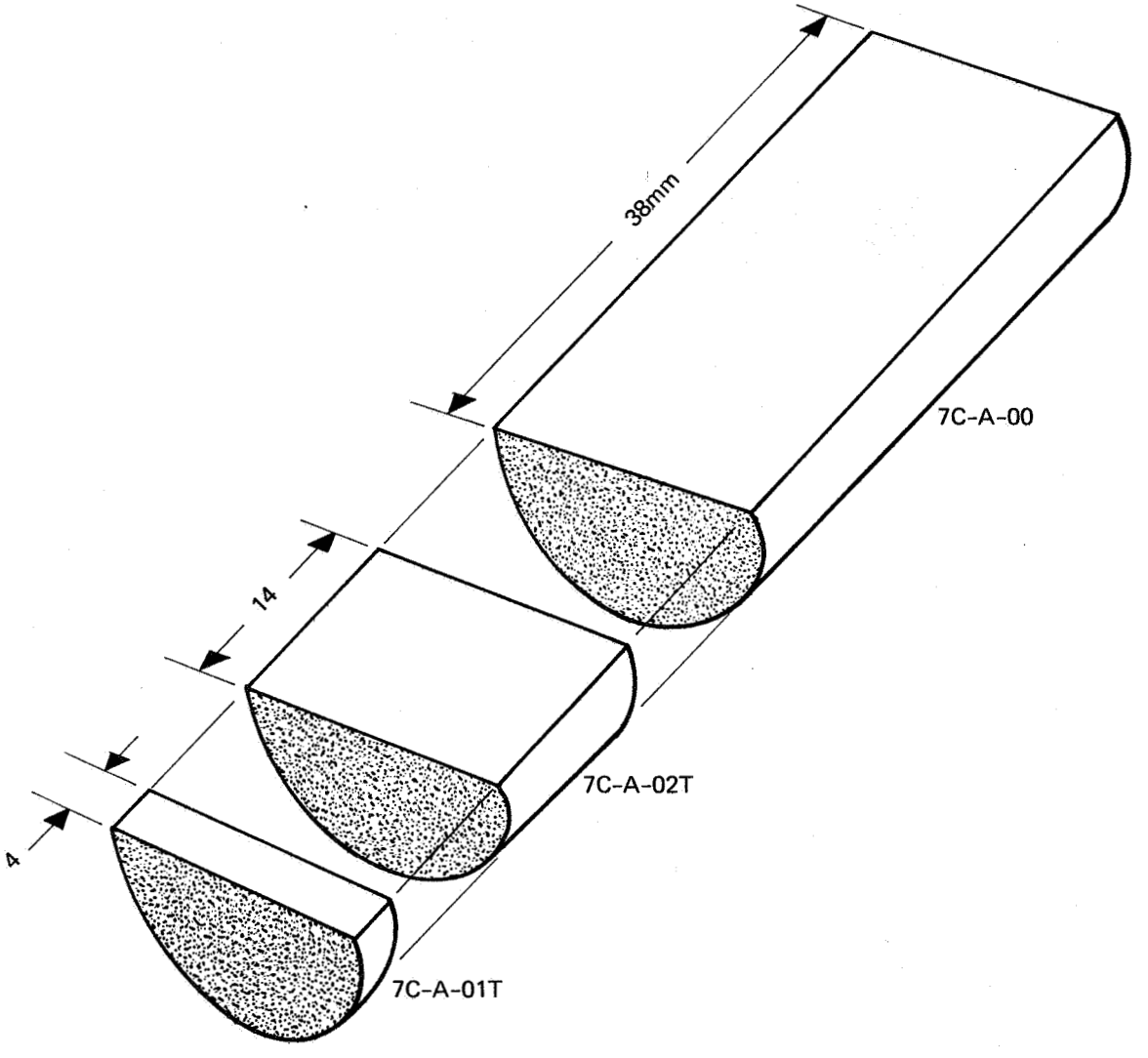

FIGURE 26 SCHEMATIC SKETCH OF SAMPLE SECTIONS FROM 7C-A-00

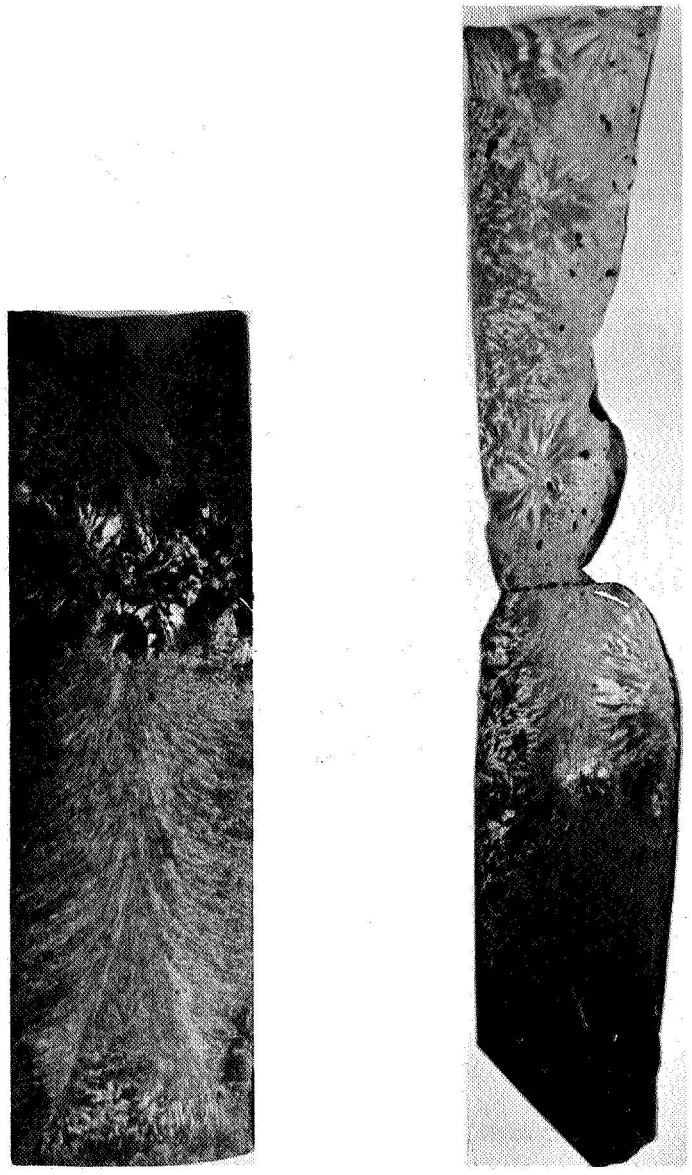

7C-A-00 7F-A-00

(Heat Sink End)

FIGURE 27 MACROPHOTOGRAPHS OF LONGITUDINAL SECTIONS, SAMPLES NO. 7C AND 7F, ETCHED, 2x

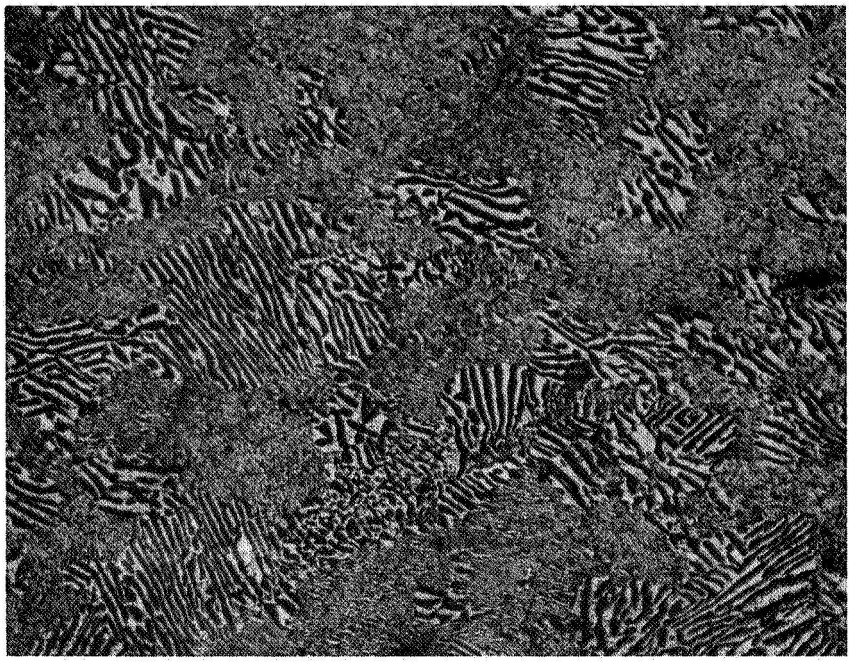

a) Fine Lamellar Colonies 125x

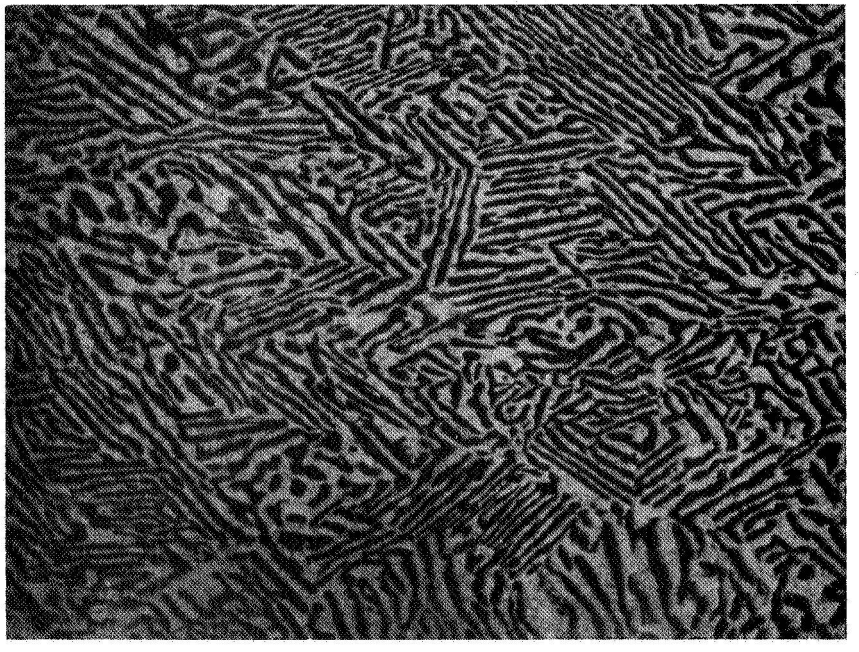

b) "Chinese Script" 250x

FIGURE 28 STRUCTURAL FEATURES OBSERVED IN SAMPLE 7C-A-00, ETCHED

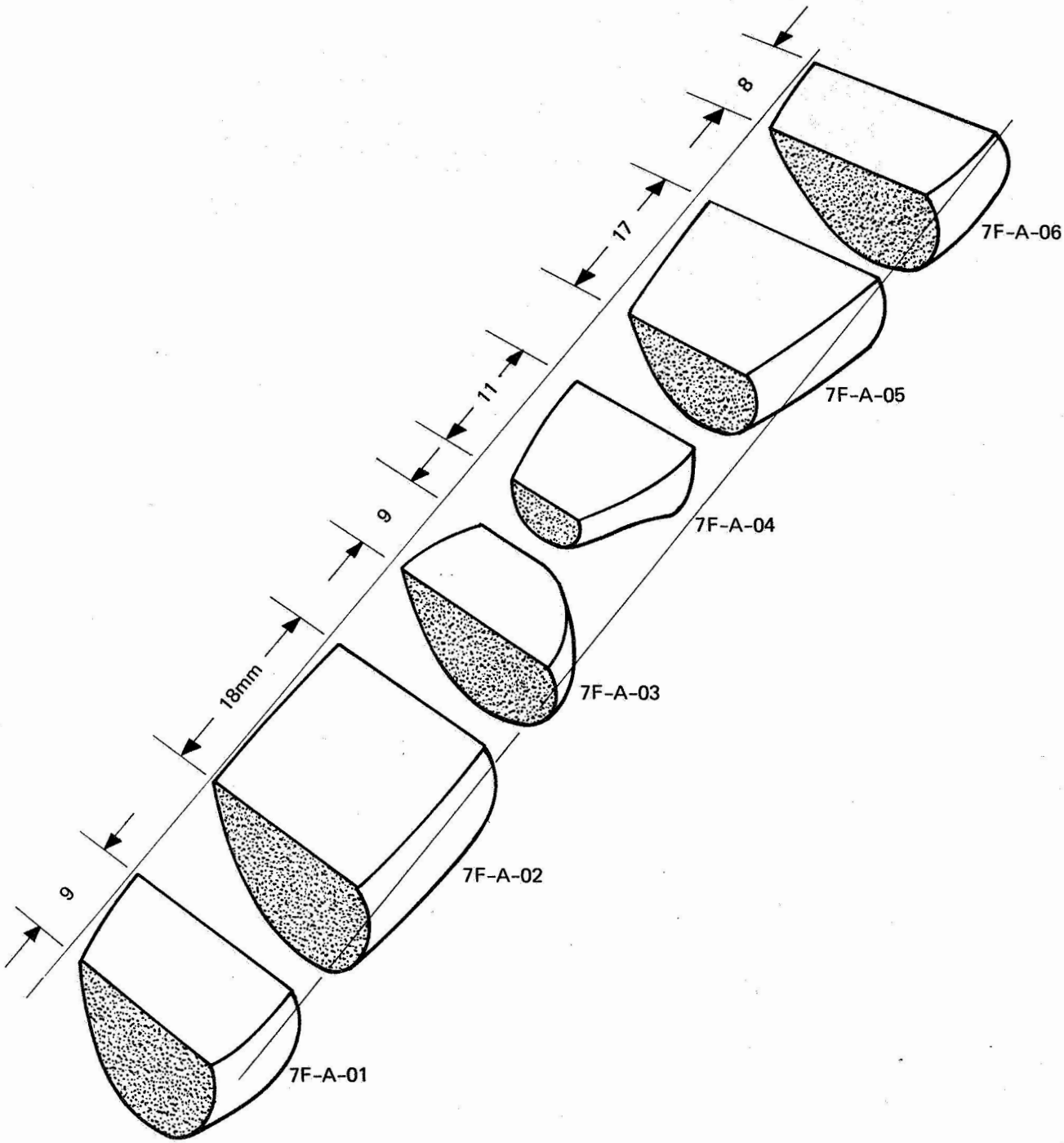

FIGURE 29 SCHEMATIC SKETCH OF SAMPLE SECTIONS FROM 7F-A-00

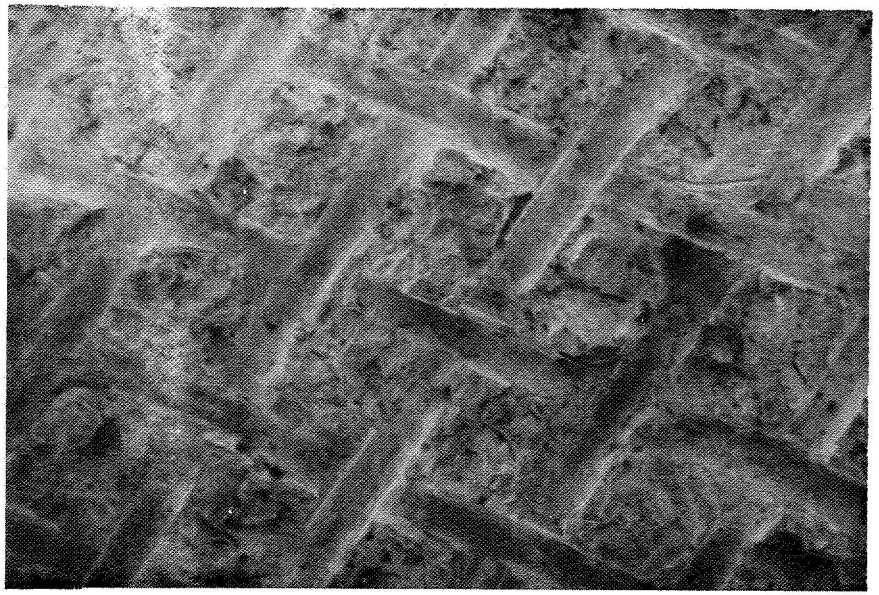

733–1 30x

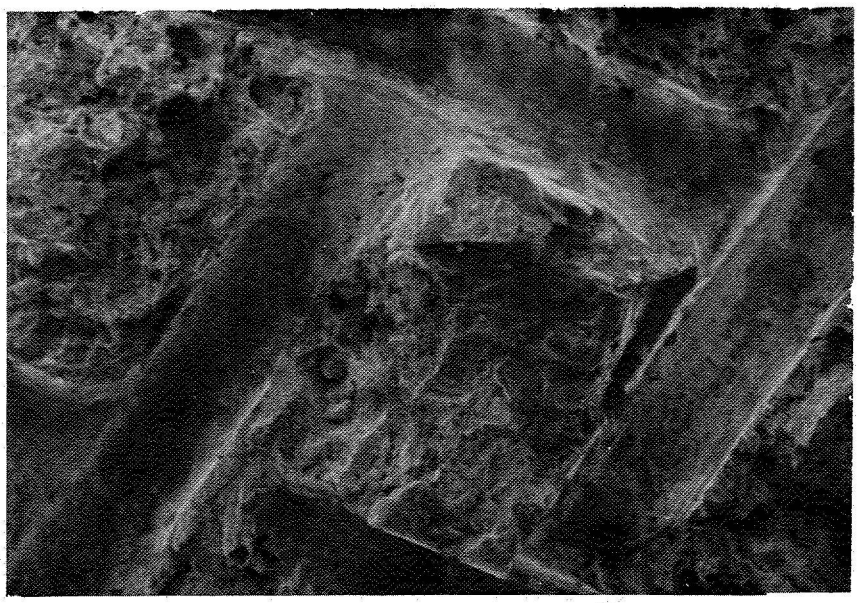

733–4 75x

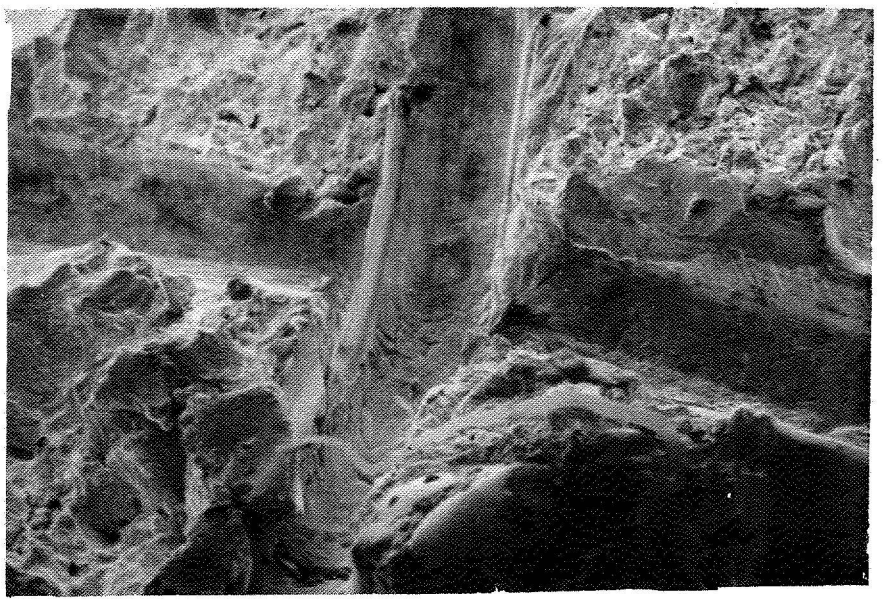

733–5 400x

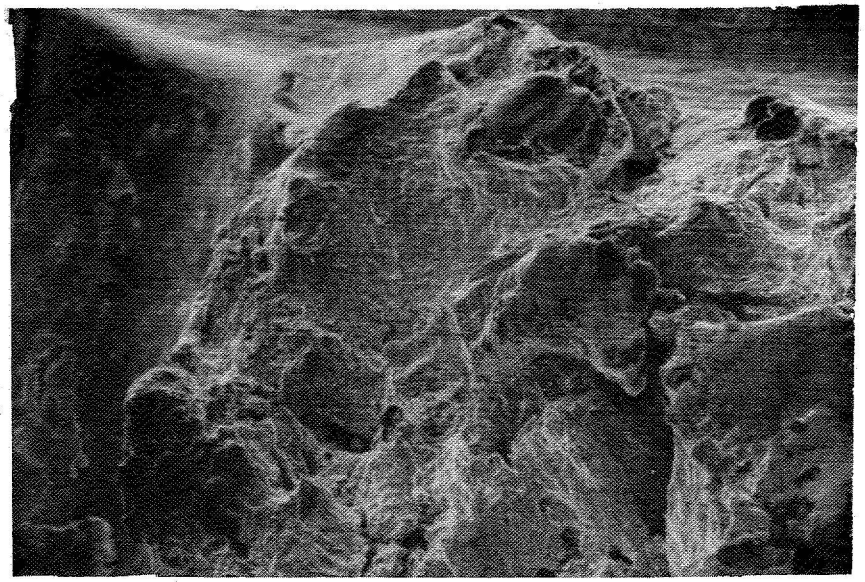

733–6 790x

FIGURE 30 SCANNING ELECTRON MICROGRAPHS OF FRACTURED SURFACE ADJACENT TO STAINLESS STEEL SCREEN, SAMPLE 7F-A-03

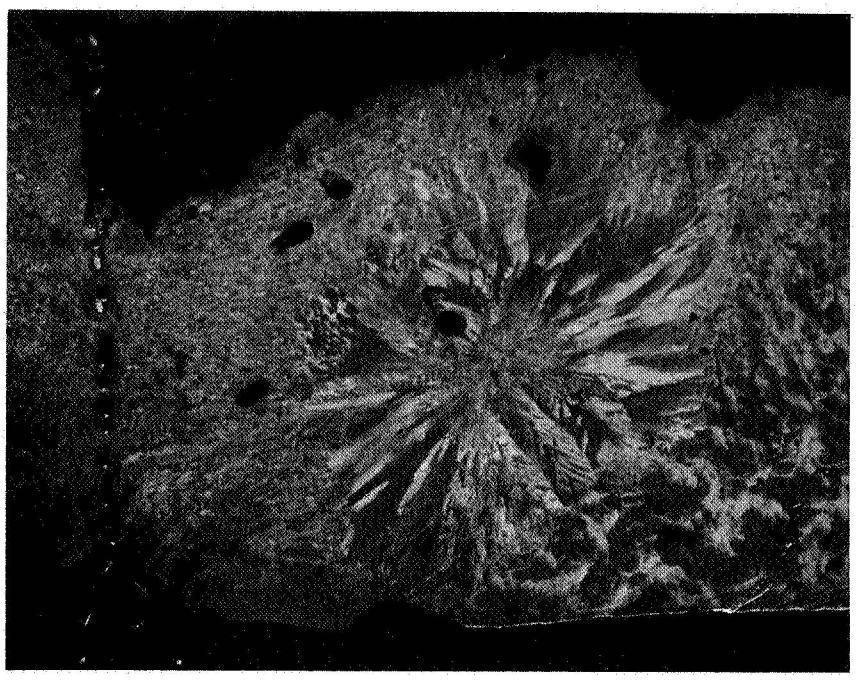

8x

FIGURE 31 ROSETTE STRUCTURE OBSERVED IN SAMPLE 7F-A-00, ETCHED

a) Core of Rosette 65x

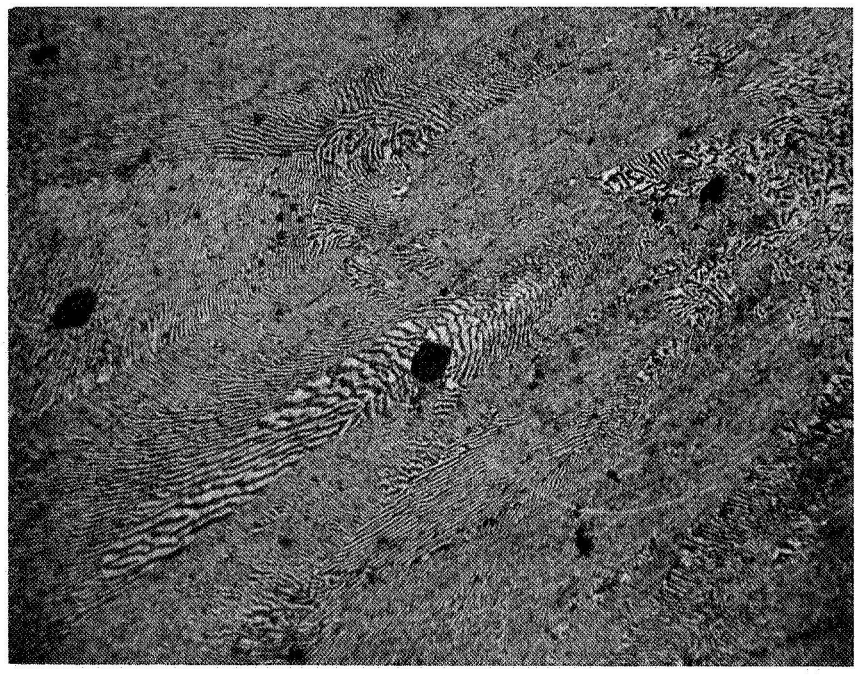

b) Rosette Petal 65x

FIGURE 32 STRUCTURE WITHIN A ROSETTE, SAMPLE 7F-A-00, ETCHED

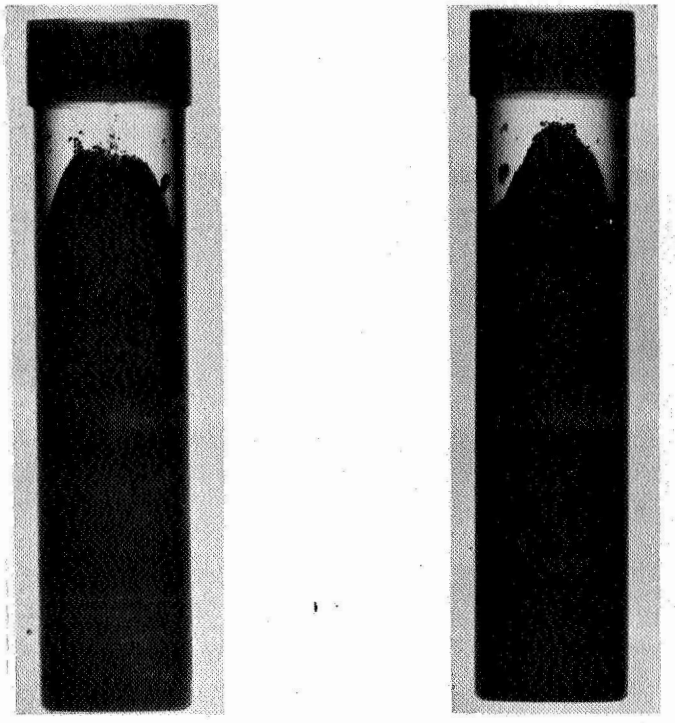

0° 90°

FIGURE 33 X–RAY RADIOGRAPHS OF SAMPLE 8C

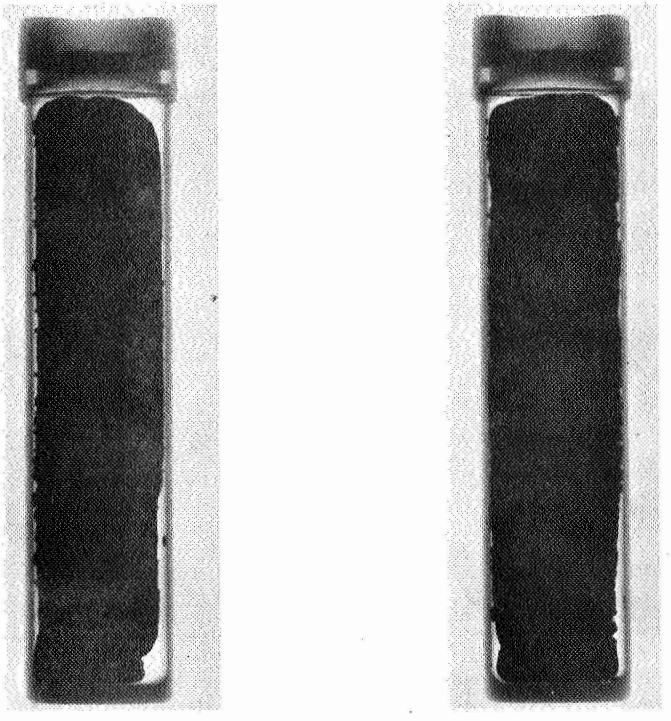

0° 90°

FIGURE 34 X–RAY RADIOGRAPHS OF SAMPLE 8F

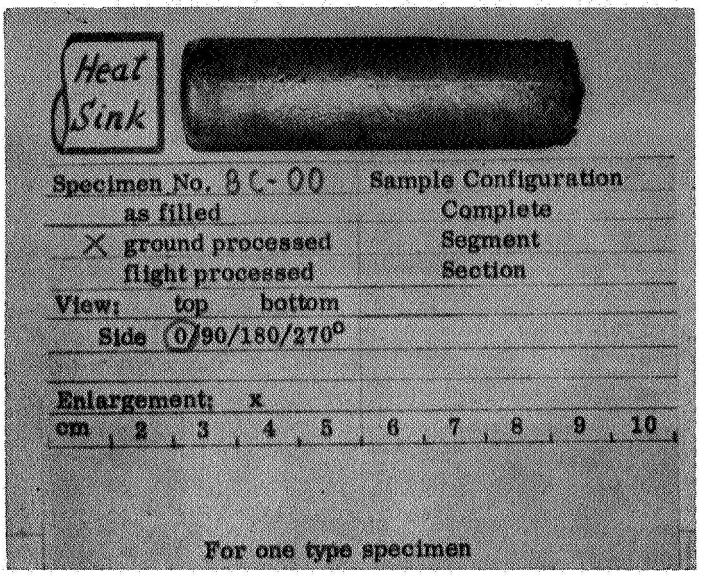

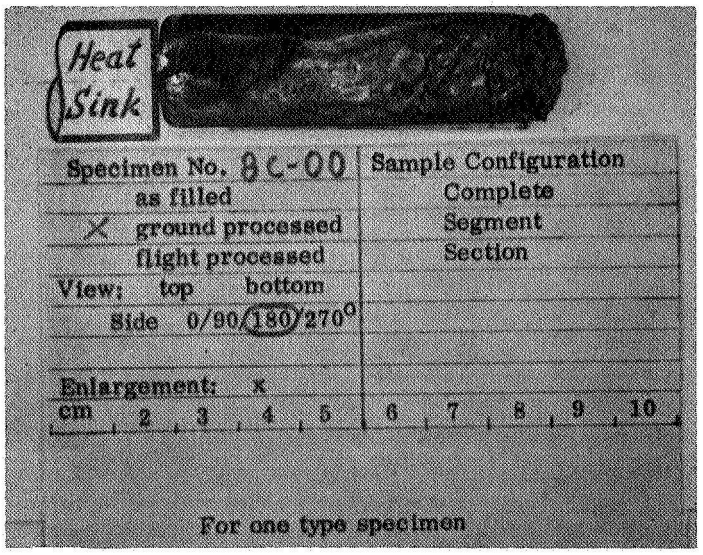

FIGURE 35 SIDE VIEWS OF SAMPLE NO. 8C-00 AFTER REMOVAL FROM CAPSULE

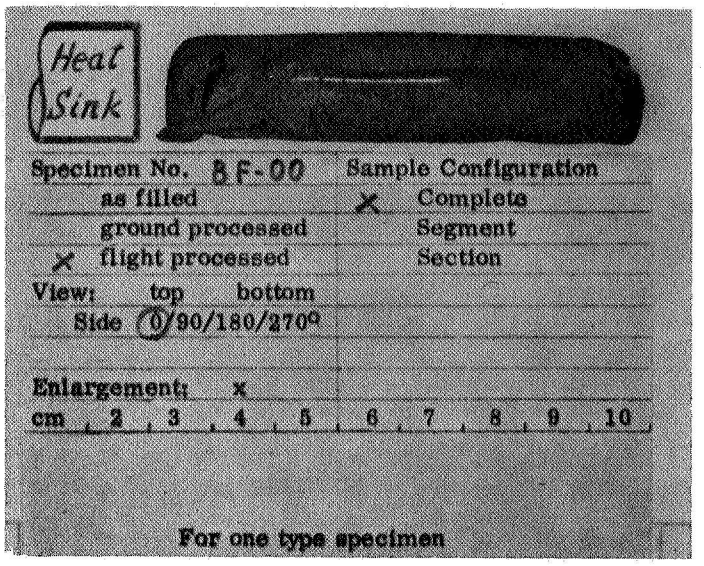

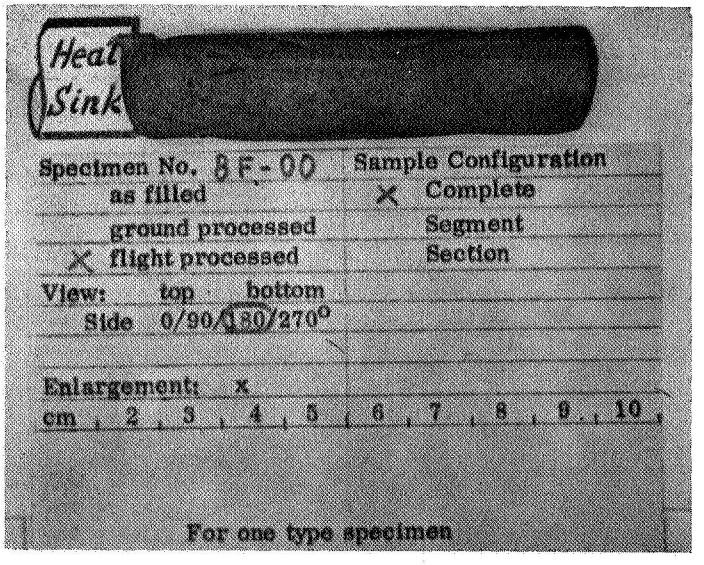

FIGURE 36 SIDE VIEWS OF SAMPLE NO. 8F-00 AFTER REMOVAL FROM CAPSULE

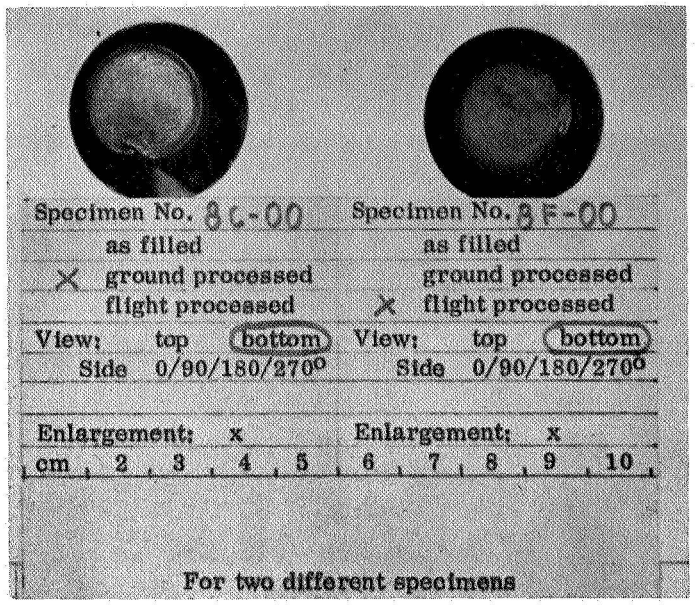

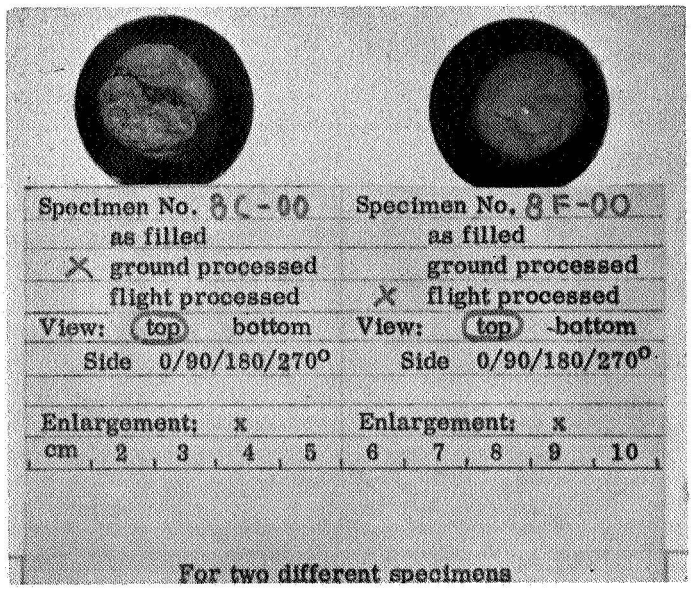

FIGURE 37 END VIEWS OF SAMPLES 8C-00 AND 8F-00 AFTER REMOVAL FROM CAPSULE

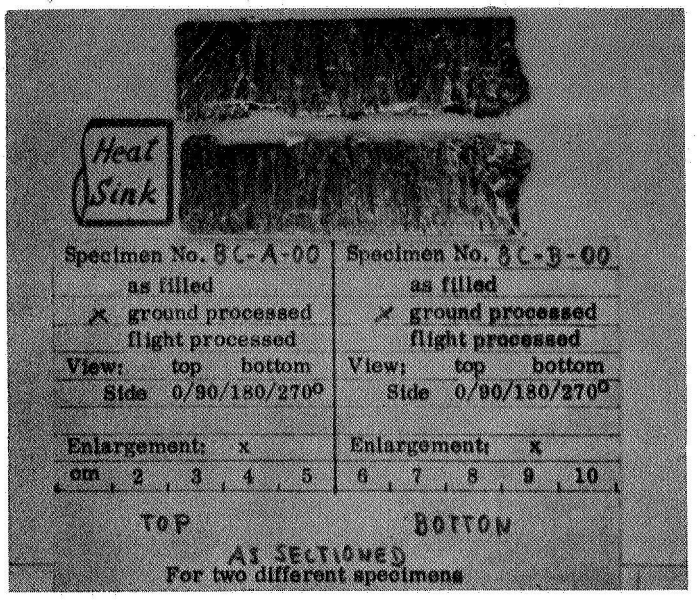

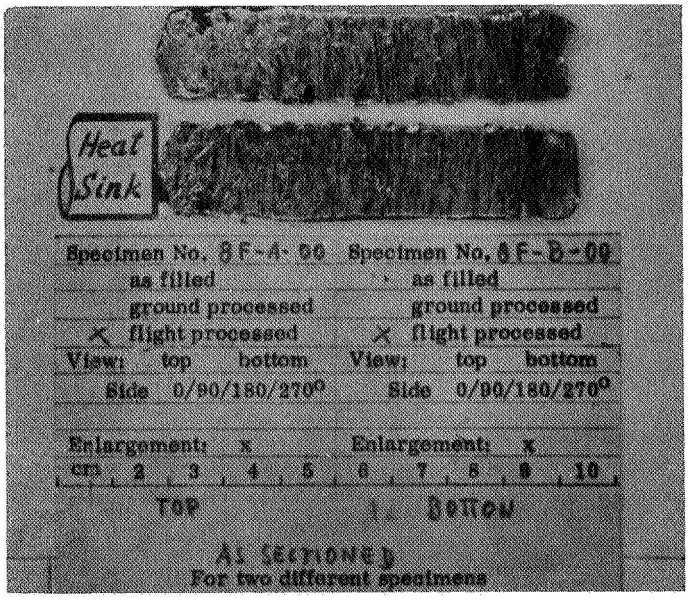

FIGURE 38 PHOTOGRAPHS OF LONGITUDINAL SECTION OF SAMPLES 8C-00 AND 8F-00

8C-A-00 8F-A-00

(Heat Sink End)

FIGURE 39 MACROPHOTOGRAPHS OF LONGITUDINAL SECTIONS, SAMPLES NO. 8C AND 8F, ETCHED, 2x

~25x

FIGURE 40 TUNGSTEN SPHERES EMBEDDED IN EXTERNAL SURFACE OF SAMPLE 8C-A-00

65x

FIGURE 41 PRIMARY In_2Bi DENDRITES PRESENT IN SAMPLE 8C-A-00

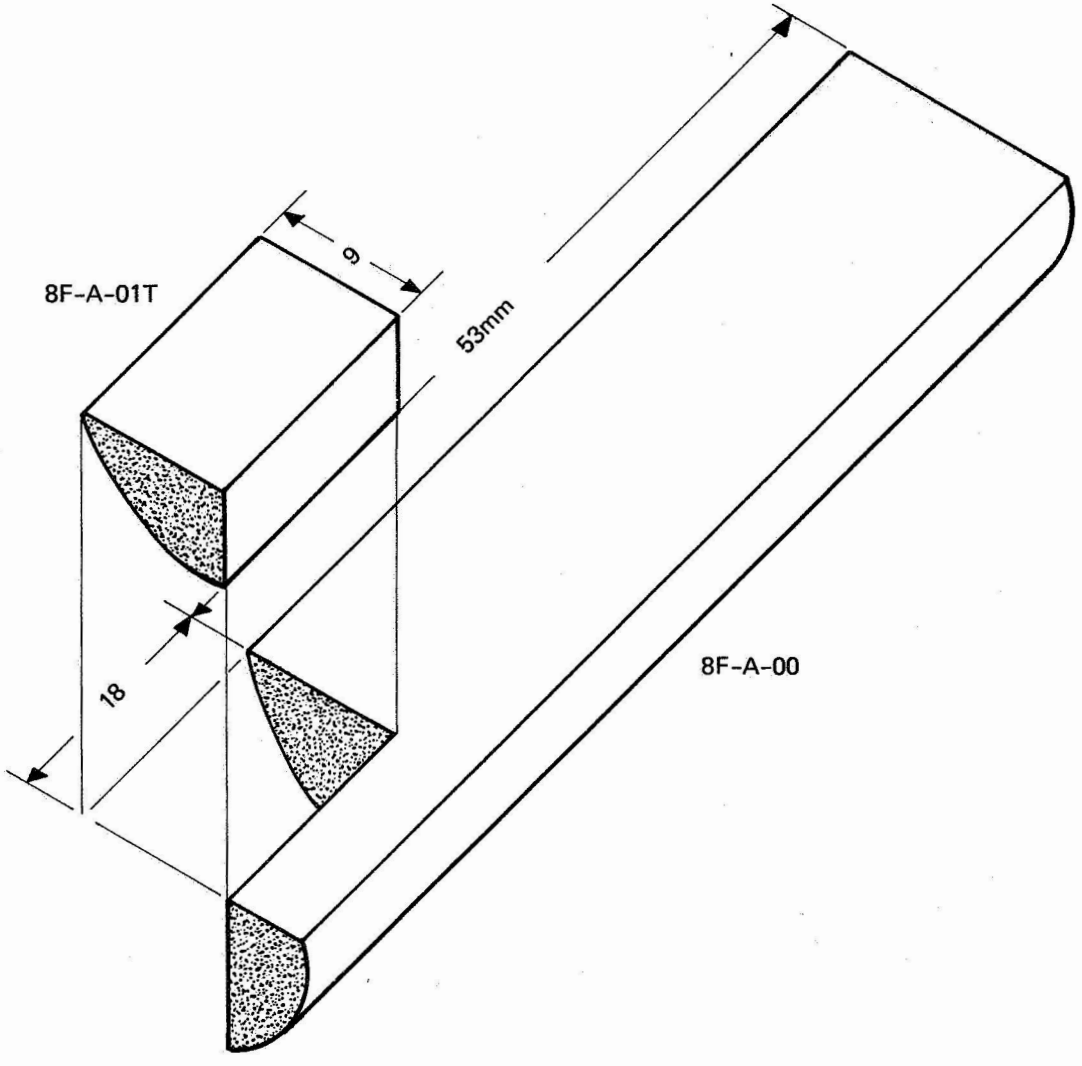

FIGURE 42 SCHEMATIC SKETCH OF SAMPLE SECTIONS FROM 8F-A-00

∿ 20X

FIGURE 43 PHOTOGRAPH SHOWING DISTRIBUTION OF TUNGSTEN SPHERES IN PORES, SAMPLE 8F-A-00

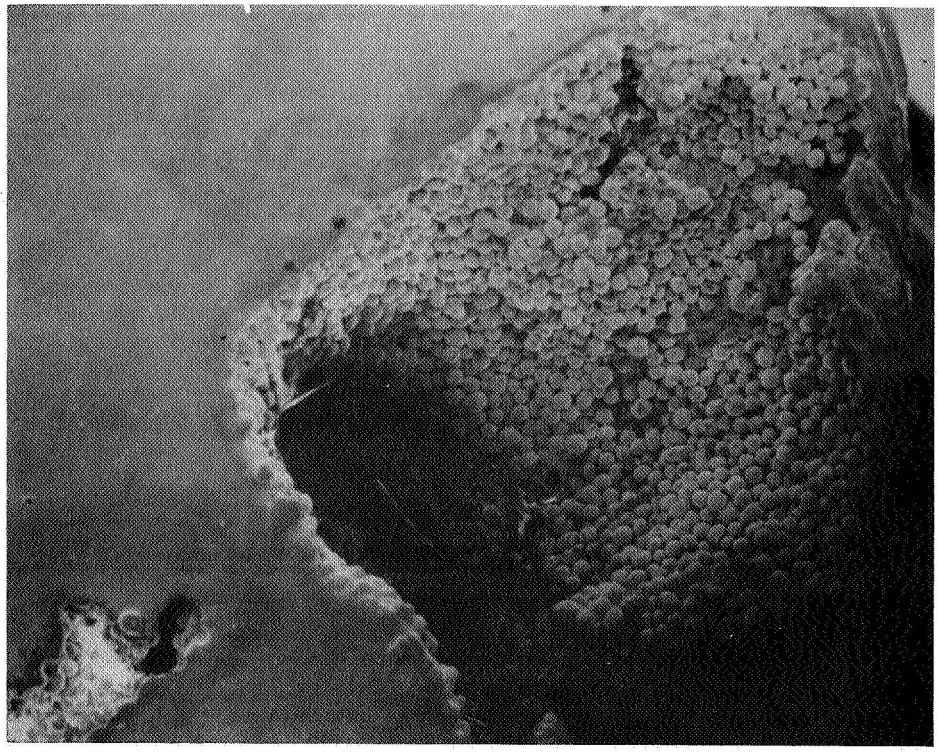

714–1 ∿ 40X

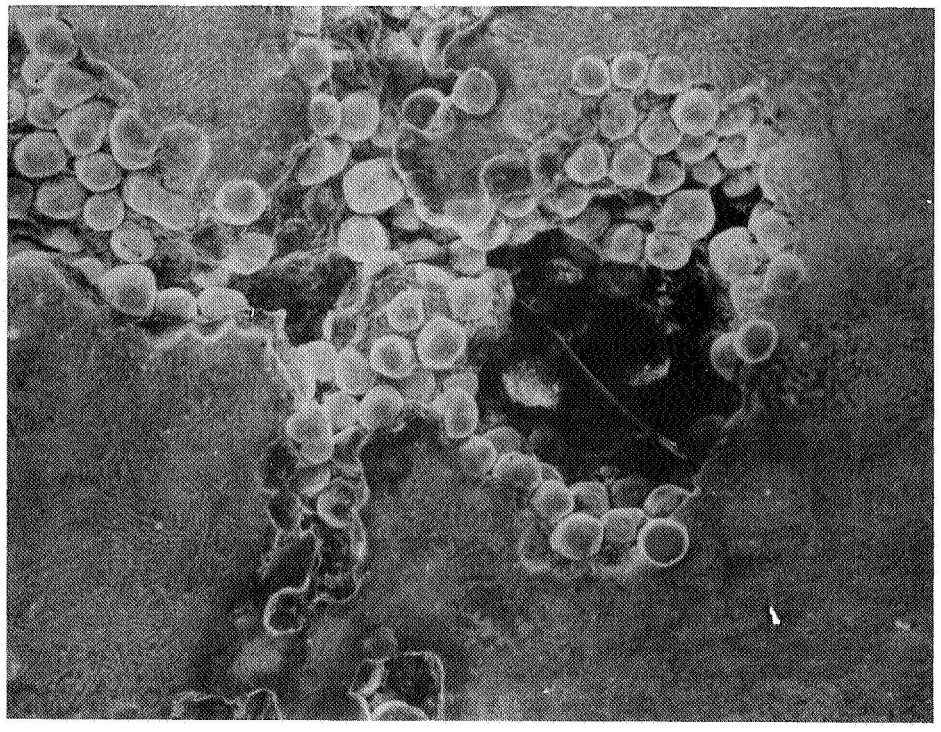

714–5 ∿ 120X

FIGURE 44 SCANNING ELECTRON MICROGRAPHS SHOWING DISTRIBUTION OF TUNGSTEN SPHERES IN SAMPLE NO. 8F-A-00

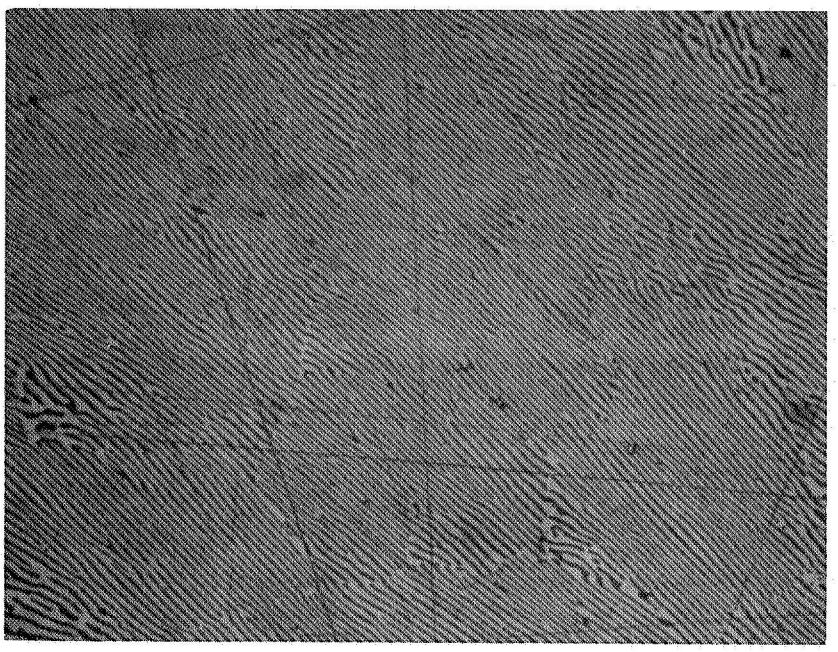

250x

FIGURE 45 ALIGNED LAMELLAR EUTECTIC PRESENT IN AREAS OF SAMPLE 8F-A-00, ETCHED

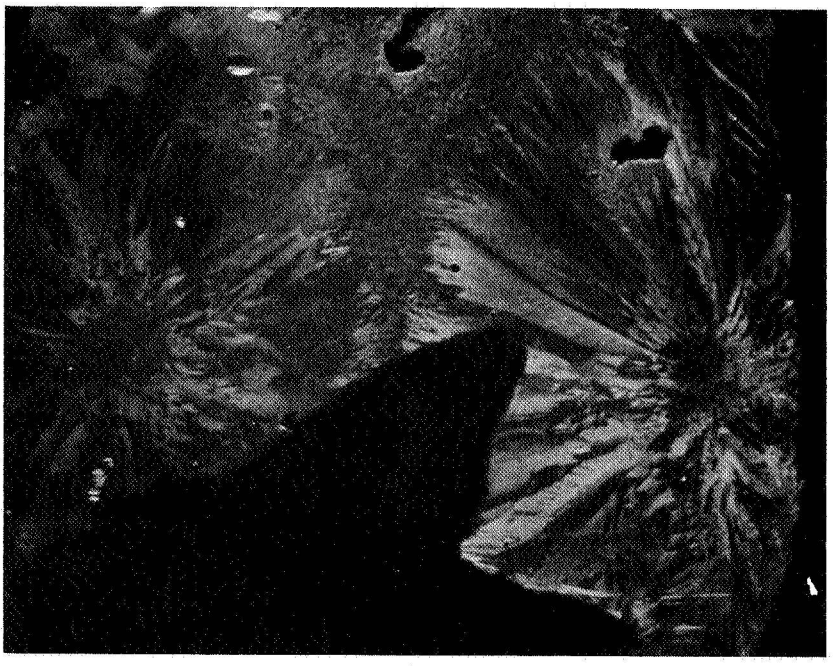

8x

FIGURE 46 ROSETTE STRUCTURE OBSERVED IN SAMPLE 8F-A-00, ETCHED

TECHNICAL REPORT STANDARD TITLE PAGE

1. REPORT NO.	2. GOVERNMENT ACCESSION NO.	3. RECIPIENT'S CATALOG NO.
NASA CR-61369		

4. TITLE AND SUBTITLE	5. REPORT DATE
APOLLO 14 COMPOSITE CASTING DEMONSTRATION Final Report	August 20, 1971 6. PERFORMING ORGANIZATION CODE
7. AUTHOR(S)	8. PERFORMING ORGANIZATION REPORT #
9. PERFORMING ORGANIZATION NAME AND ADDRESS Arthur D. Little, Inc. Cambridge, Mass. 02140	10. WORK UNIT NO. 11. CONTRACT OR GRANT NO. NAS 8-26637
12. SPONSORING AGENCY NAME AND ADDRESS National Aeronautics and Space Administration Washington, D. C. 20546	13. TYPE OF REPORT & PERIOD COVERED Contractor Report Final 14. SPONSORING AGENCY CODE

15. SUPPLEMENTARY NOTES

Technical Monitor: Iva C. Yates, PT Laboratory, George C. Marshall Space Flight Center

16. ABSTRACT

The objective of this program is to assist in the design and implementation of the Composite Casting Demonstration for the Apollo 14 mission. Both flight and control samples were evaluated.

Some conclusions resulting from a comparison of the flight and control samples are as follows:

1. Solidification in neither the flight nor control samples was truly directional.
2. Apparent intermittent contact of the melt with the container in the flight samples led to unusual nucleation and growth structures.
3. There was greater uniformity, on a macro scale, of both pores and structural features in the flight sample; presumably the result of the reduced gravity conditions.
4. It seems quite feasible to produce enhanced dispersions of gases and dense phases in a melt which is solidified in reduced gravity.
5. A two-stage heating/cooling cycle may help directional solidification.
6. Sample materials should be selected from materials in which the dispersant fully wets the matrix material.
7. Experiments should be conducted in two modes: (1) where the melt is in good thermal contact with the container, and (2) where the melt is in a free-float condition.

17. KEY WORDS	18. DISTRIBUTION STATEMENT
	Iva C. Yates, Jr. Unclassified-unlimited

19. SECURITY CLASSIF. (of this report)	20. SECURITY CLASSIF. (of this page)	21. NO. OF PAGES	22. PRICE
U	U	94	$3.00

MSFC - Form 3292 (May 1969)